Latest results on Soft QCD and DPS from the CMS experiment

Rajat Gupta
On behalf of CMS Collaboration

Panjab University Chandigarh (India)
EDS Blois 2019, XVth Rencontres du Vietnam,
June 23-29, 2019, ICISE, Quy Nhon, Vietnam

Outline

- Introduction
- MB Measurements
- UE Measurements
- DPS Measurements
- Summary

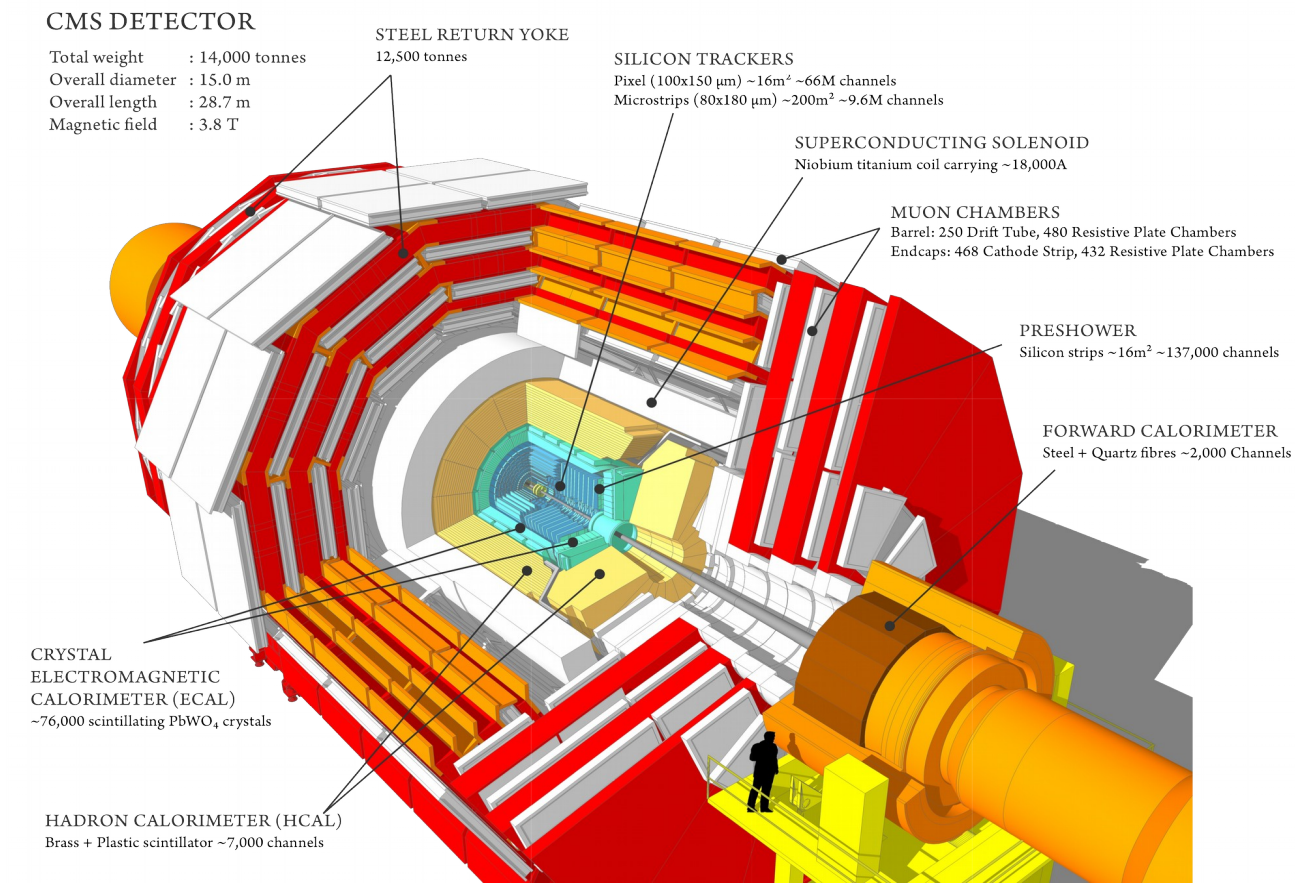

Introduction

- Soft interactions : interactions with low transverse momentum exchange where perturbative approach is not applicable

- Area includes:
  - **Minimum Bias Events**
  - **Total and inelastic pp cross section**

$$\sigma_{tot}(s) = \sigma_{el}(s) + \sigma_{inel}(s).$$

$$\boxed{\sigma_{inel}(s) = \sigma_{sd}(s) + \sigma_{dd}(s) + \sigma_{cd}(s) + \sigma_{nd}(s).}$$

  - **Diffraction**
  - **Fragmentation/Hadronization**
  - **Underlying event** : additional activity on top of hard scattering

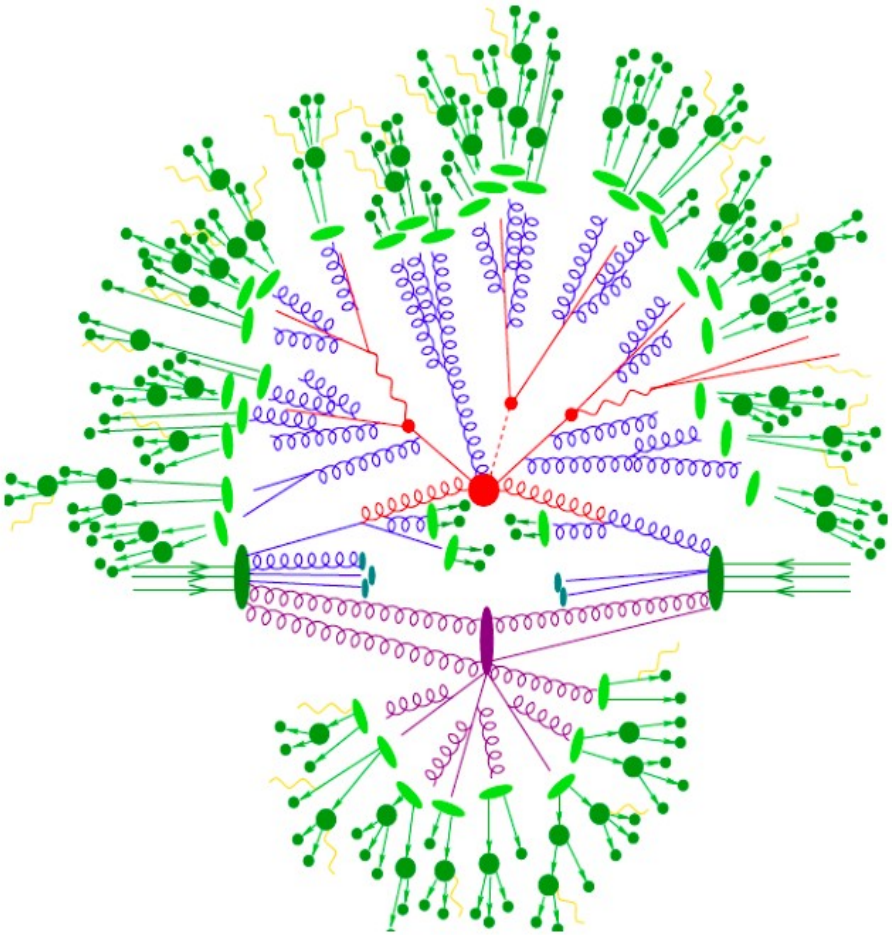

Main Interaction

Radiation (ISR/FSR)

Fragmentation/Hadronization

Multiple Interactions (MPI)

Beam remnant

Soft QCD and DPS Analysis in CMS

- inclusive very forward jet cross sections Measurement NEW
- average very forward energy as a function of the track multiplicity measurement NEW
- Charged-particle spectra in MB events
- underlying event in $t\bar{t}$ dilepton events
- DPS measurements in same sign WW at 13 TeV NEW
- Extraction and validation of a new set of CMS PYTHIA8 tunes from UE measurements
- inelastic pp cross section BACKUP
- Bose-Einstein Correlations of Charged Hadrons BACKUP
- UE Measurement using Leading Jets and particles BACKUP
- UE measurements using Drell-Yan process BACKUP

The CASTOR Calorimeter at CMS

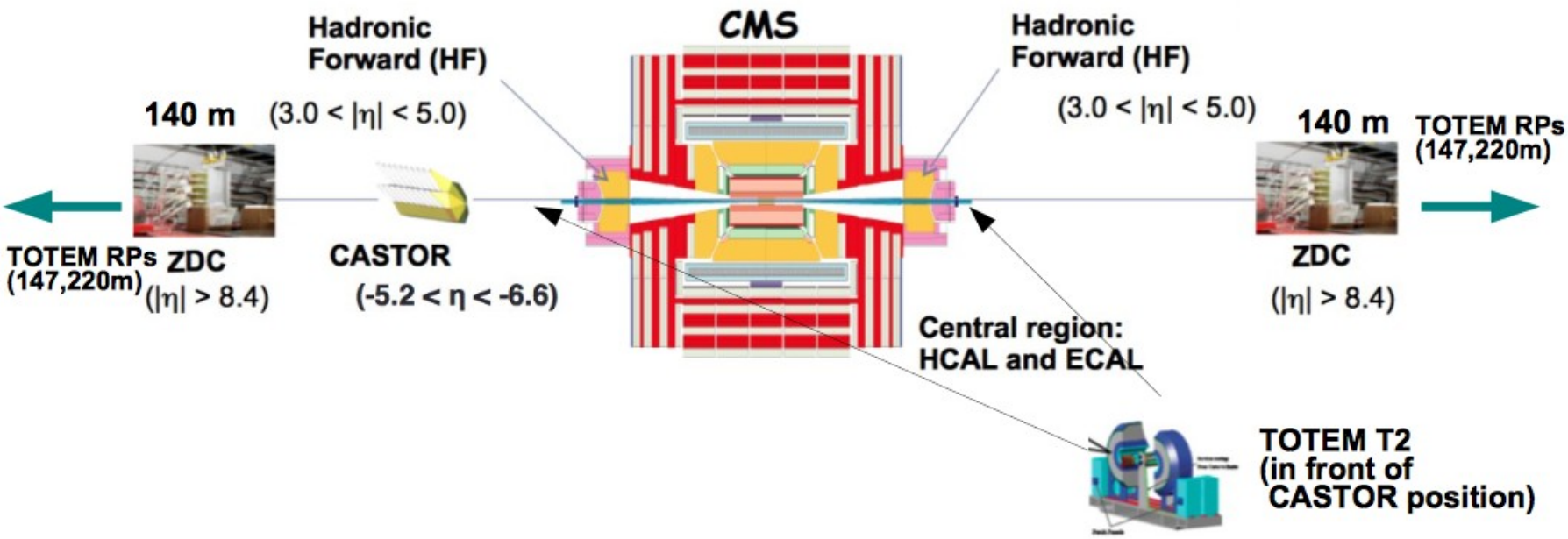

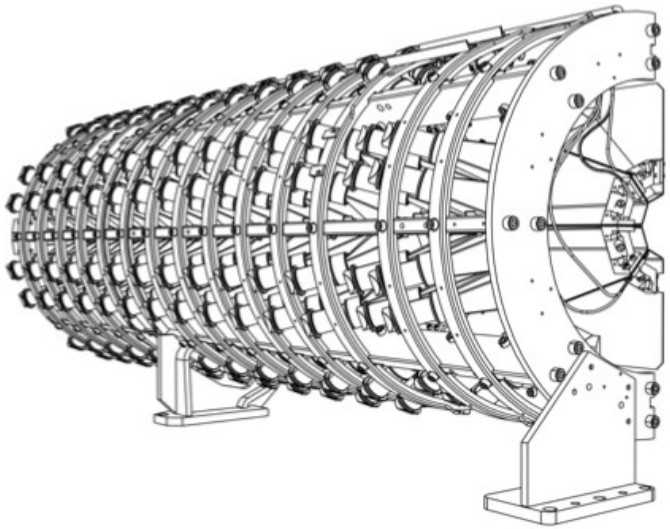

CASTOR at CMS

- CASTOR: EM-hadronic tungsten-quartz calorimeter at CMS
- Most forward conventional calorimeter deployed at the LHC, at 14 m from interaction point. Acceptance: $-6.6 \leq \eta \leq -5.2$
- Longitudinally 14-fold segmentation
- Transversally 16-fold segmentation
- CASTOR has no η segmentation! Consequence: measure energy of jets instead of p_T within its acceptance

Inclusive very forward jet cross sections in p-Pb collisions at 5.02 TeV (JHEP05(2019)043)

NEW

- differential cross sections as a function of jet energy in $-6.6 < \eta < -5.2$
- 2 type of collisions studied : either proton (p + Pb) or ion (Pb + p) traveling towards the -ve η hemisphere
- jet cross sections are unfolded to stable-particle level
- compared to predictions from various MC generators.

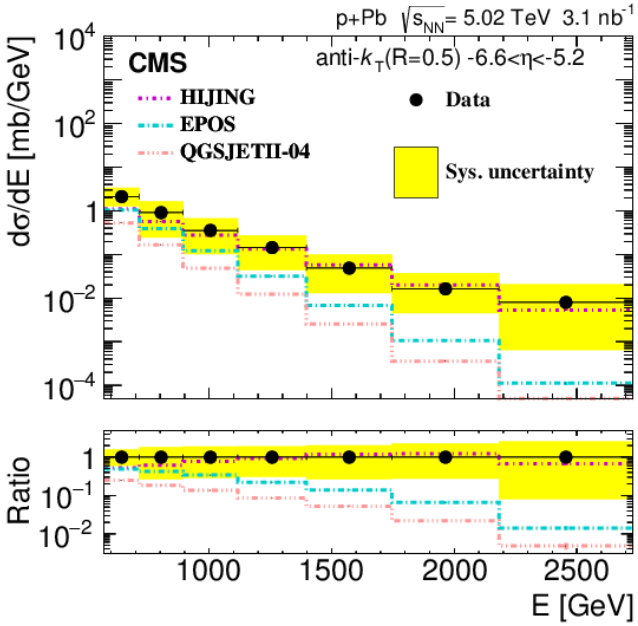

- Best described by HIJING model
- EPOS-LHC and QGSJETII-04 : both yield very soft energy spectrum and underestimate data at high energy
- Mismodeling of absolute normalization of hard scatterings in p-A collisions for EPOS-LHC improved recently
- KATIE model : “KS nonlinear” and “KS linear”
- Overall, no saturation models explain all features, & disagreement b/w data and KATIE AAMQS saturation models is largest in region where nonlinear effects are strongest

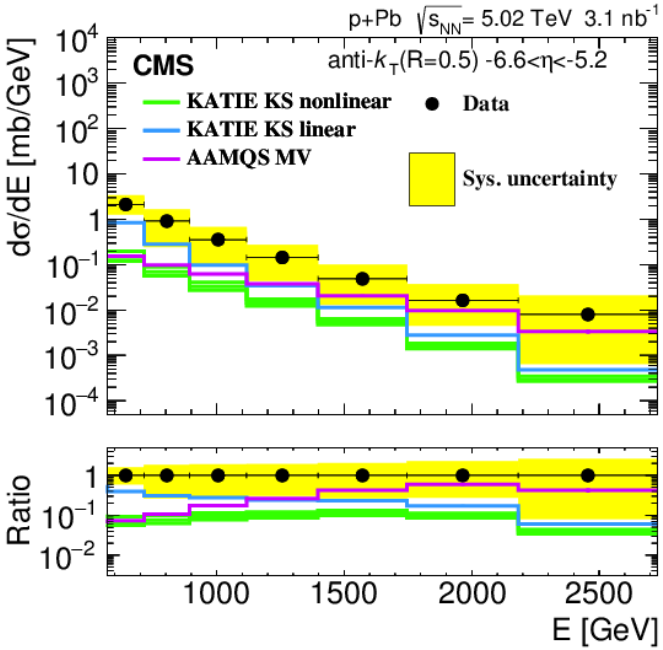

Inclusive very forward jet cross sections in p-Pb collisions at 5.02 TeV JHEP05(2019)043

NEW

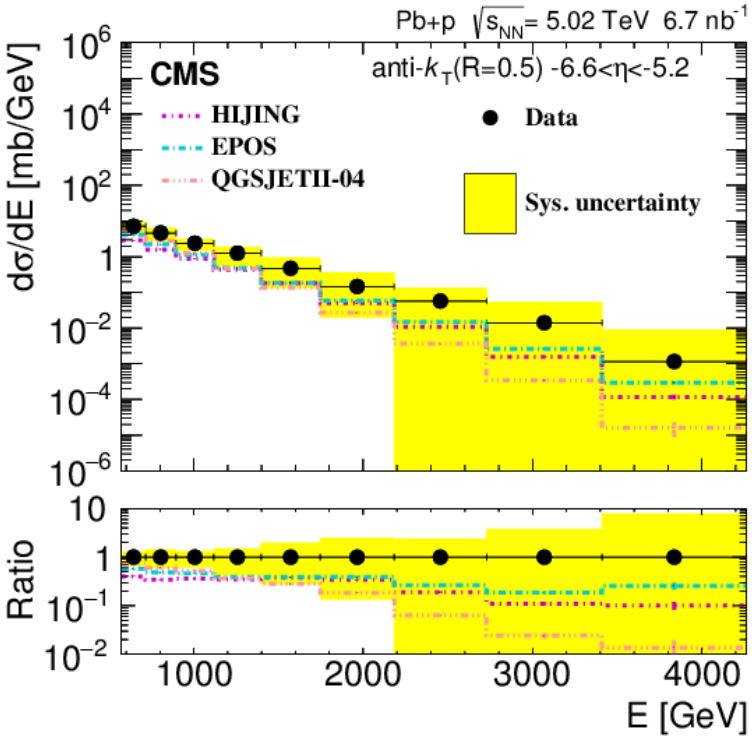

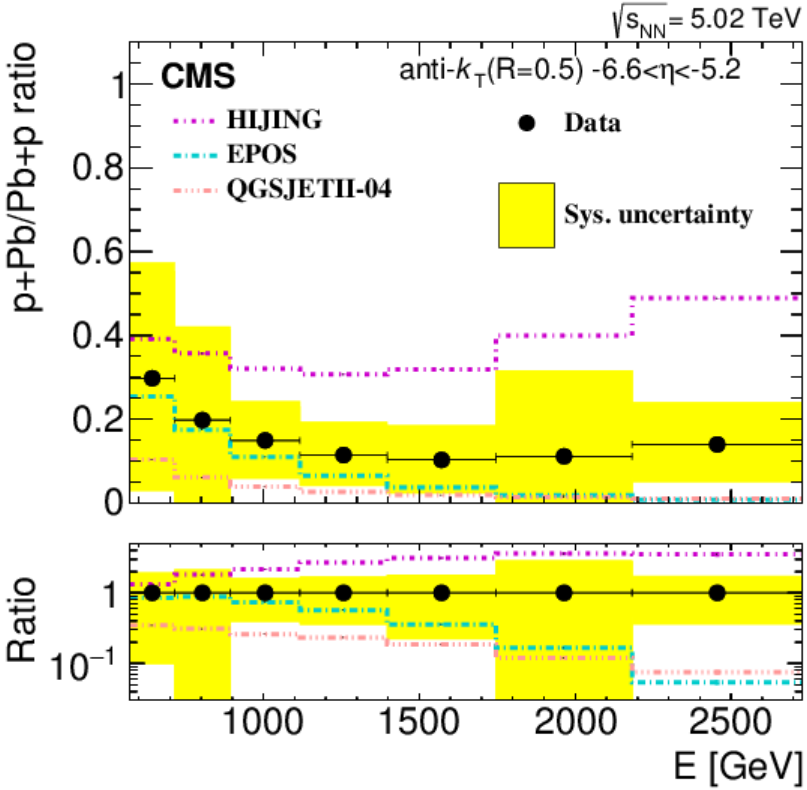

- Pb+p configuration:

  -- significant contribution from ion remnants,

  -- EPS-LHC and HIJING models describe data reasonable well, but are too low in normalization. QGSJETII-04 model yields soft spectrum.

- Ratio of p+Pb and Pb+p :
  -- None of the models describe data for whole range. The HIJING model describes shape of data best, but fails to describe its magnitude.

  -- EPOS-LHC describes lower part well, fails to describe shape at high energy
  -- QGSJETII-04 underestimates both shape and normalization of the ratio.

Average very forward energy measurement at 13 TeV (CMS PAS FSQ-18-001)

NEW

- average energy reconstructed with the CASTOR calorimeter in the region $-6.6 < \eta < -5.2$ as a function of the track multiplicity for $|\eta| < 2$
- measurement is presented in terms of the total energy as we as its EM and hadronic components.
- The very forward region covered by the data contains the highest energy densities studied in p-p collisions at the LHC.
- This makes the data in particular relevant for improving the modelling of multi particle production in event generators.

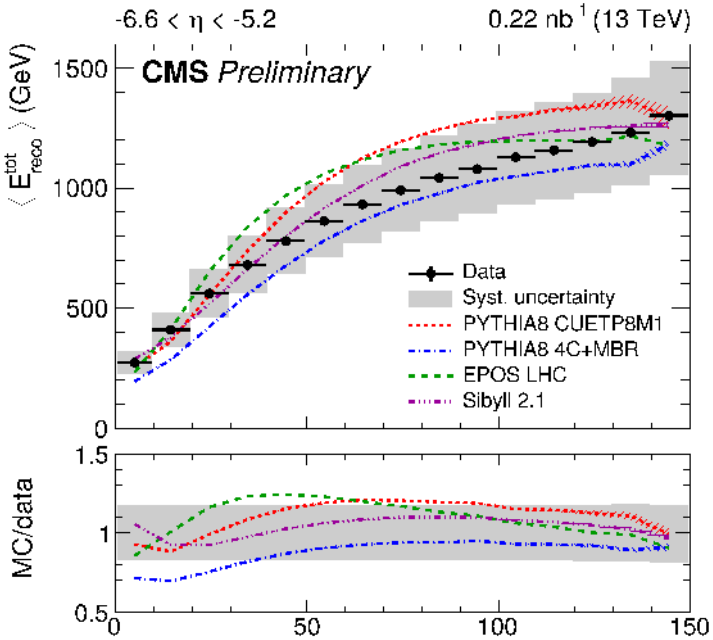

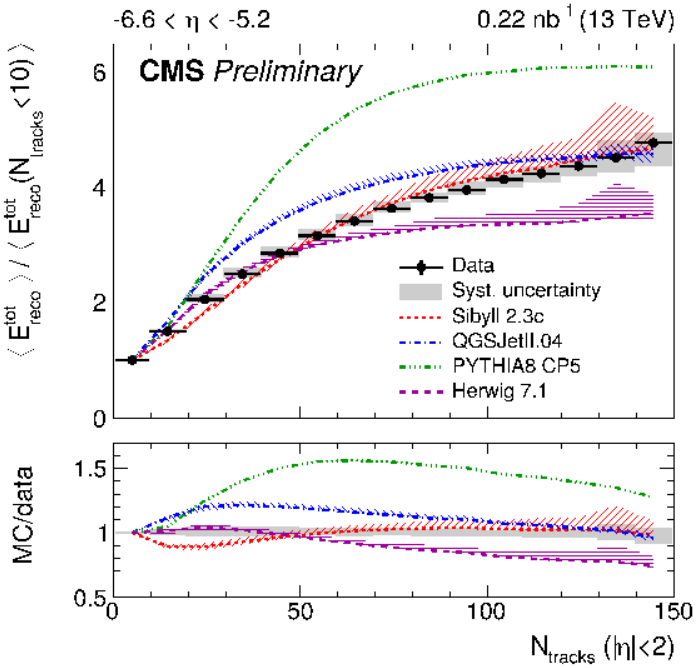

- Measured avg. total energy as function of track multiplicity is described very well by all models. Implying UE event parameter tunes performed at mid-rapdiity can be extrapolated to very forward direction.
- All P8 tunes : inconsistent, EPOS, QGSJETII : saturation above $N_{ch} > 80$
- In shape analysis, still opportunity to further improve particle production models in forward phase region. SiBYLL 2.1 shows the best agreement for multiplicity dependence of avg. Energy.

Shape comparison

Average very forward energy measurement at 13 TeV (CMS PAS FSQ-18-001)

NEW

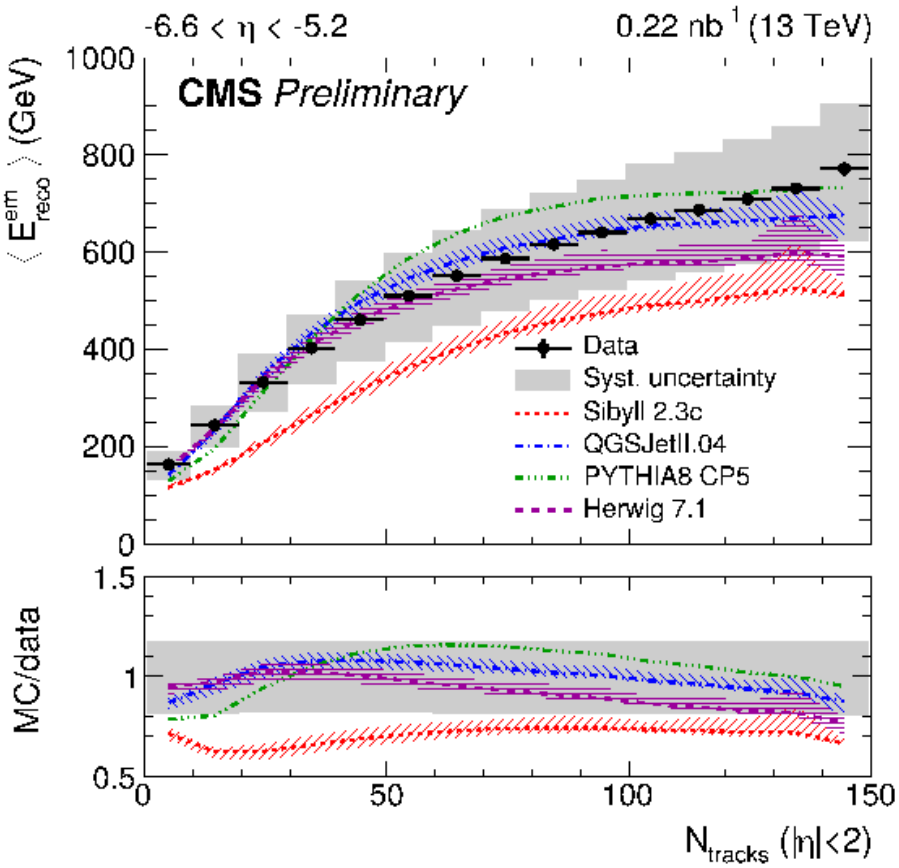

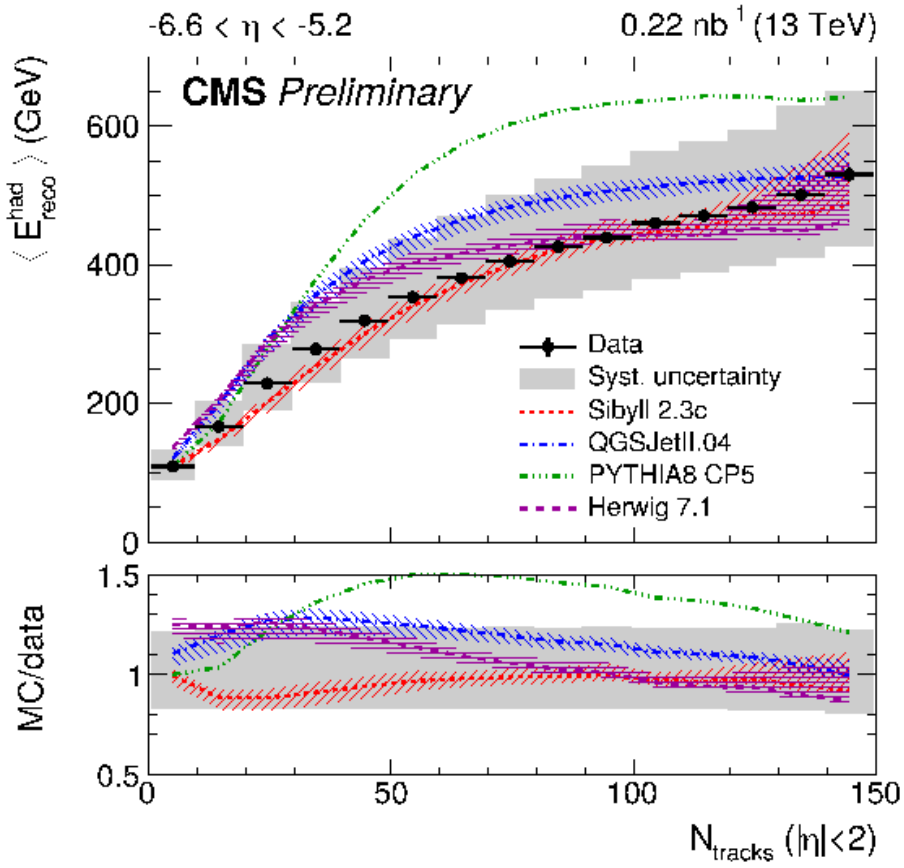

EM energy distributions:

- good description of all models Except SIBYLL 2.3c

hadronic energy distributions:

- predicted energy shows larger Spread compared to EM energy Between different models

Separate study of EM and Hadronic energy : useful to study different UE particle production

Average very forward energy measurement at 13 TeV (CMS PAS FSQ-18-001)

NEW

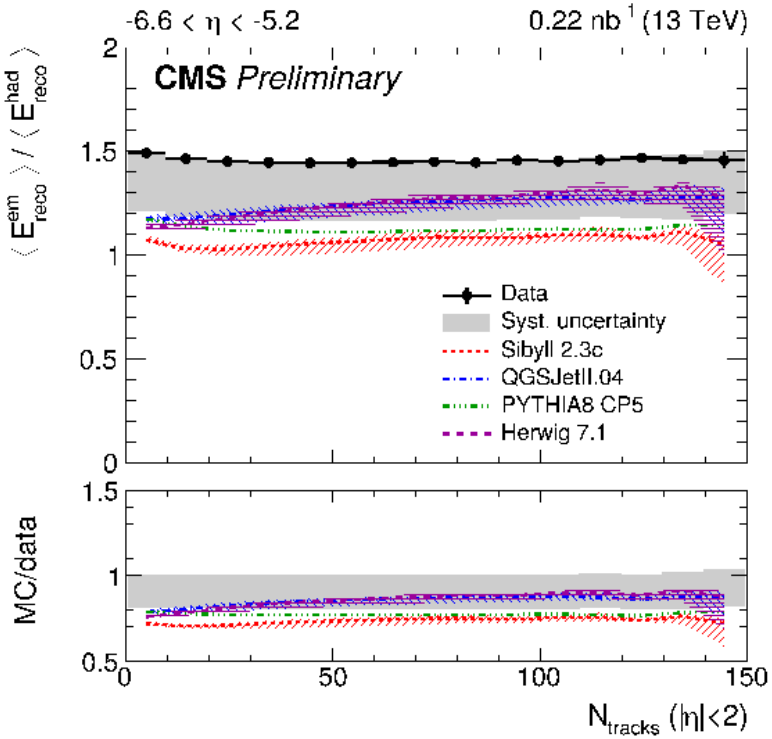

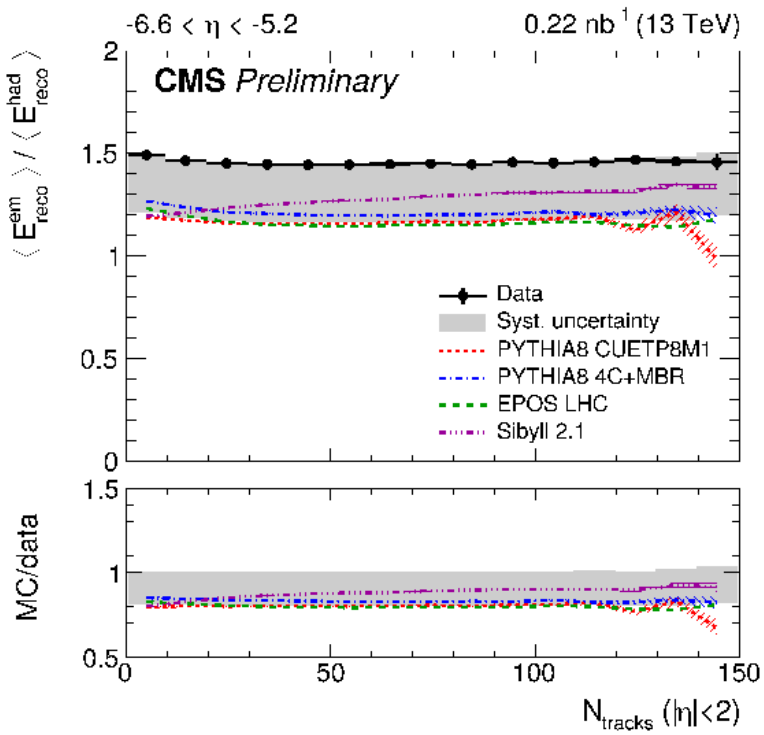

Good scope to understand string fragmentation, Remnant fragmentation, ISR/FSR/ effects of hydrodynamical phase to understand these data

- Data exhibit a larger fraction of EM energy compared to models
- disagreement with 2 recent model tunes : SIBYLL 2.3c and PYTHIA8 CP5
- This deficiency implies increased difficulty to solve muon deficit in ultra-high energy air shower simulations

Charged-particle spectra in MB events at 13 TeV
Eur. Phys. J. C (2018) 78: 697

★ : at least 1 charged particle with $p_T > 0.5$ GeV and $|\eta| < 2.4$

Activity : at least 1 particle with HF energy threshold (E) > 5 GeV

Veto : no particle with HF energy threshold (E) > 5 GeV

- Three different event selections based on activity in forward region

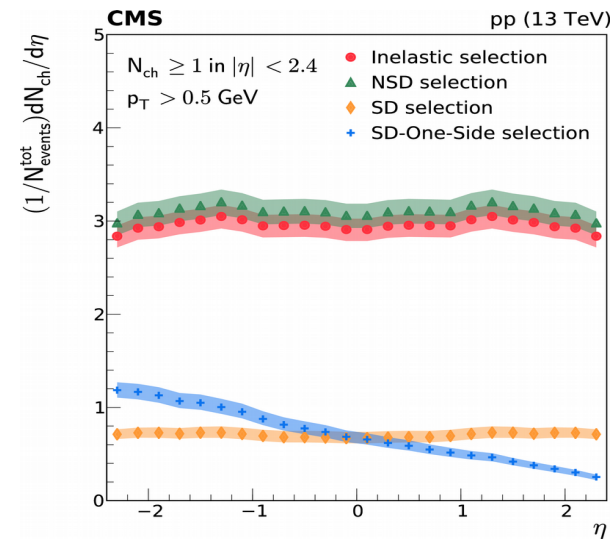

- Inelastic enhanced : ★ + Activity in at least one Fwd. region
- NonSingle Diffractive (NSD) enhanced : ★ + Activity in both Fwd. Regions
- Single Diffractive (SD) enhanced : ★ + Activity in one Fwd. Region and Veto in the other side

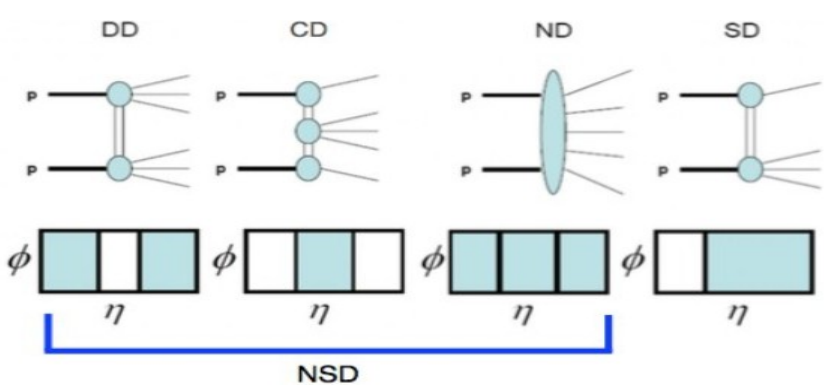

Motivation:

- Study the different components of particle production
- Constrain and tune the models
- Study transition from perturbative to non perturbative region

Charged-particle spectra in MB events at 13 TeV

- For NSD-enhanced : EPOS LHC and P8 CUETM1 give reasonable description within uncertainty
- SD-enhanced event : EPOS LHC underestimate data and P8 CUETM1 overestimate, whereas P8 MBR 4C describe the data well within uncertainty
- For charged particle multiplicity distributions, different event generators show similar prediction for inelastic and NSD events
- Room for improvement in high multiplicity regions (dominated by MPI)

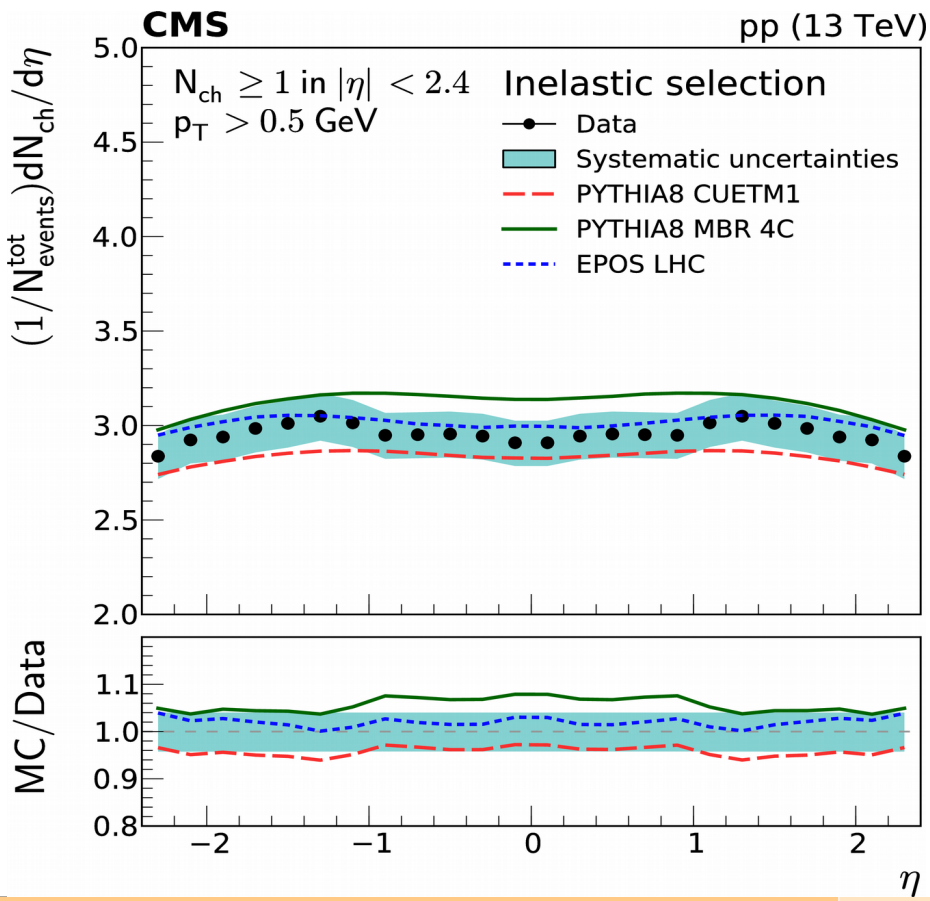

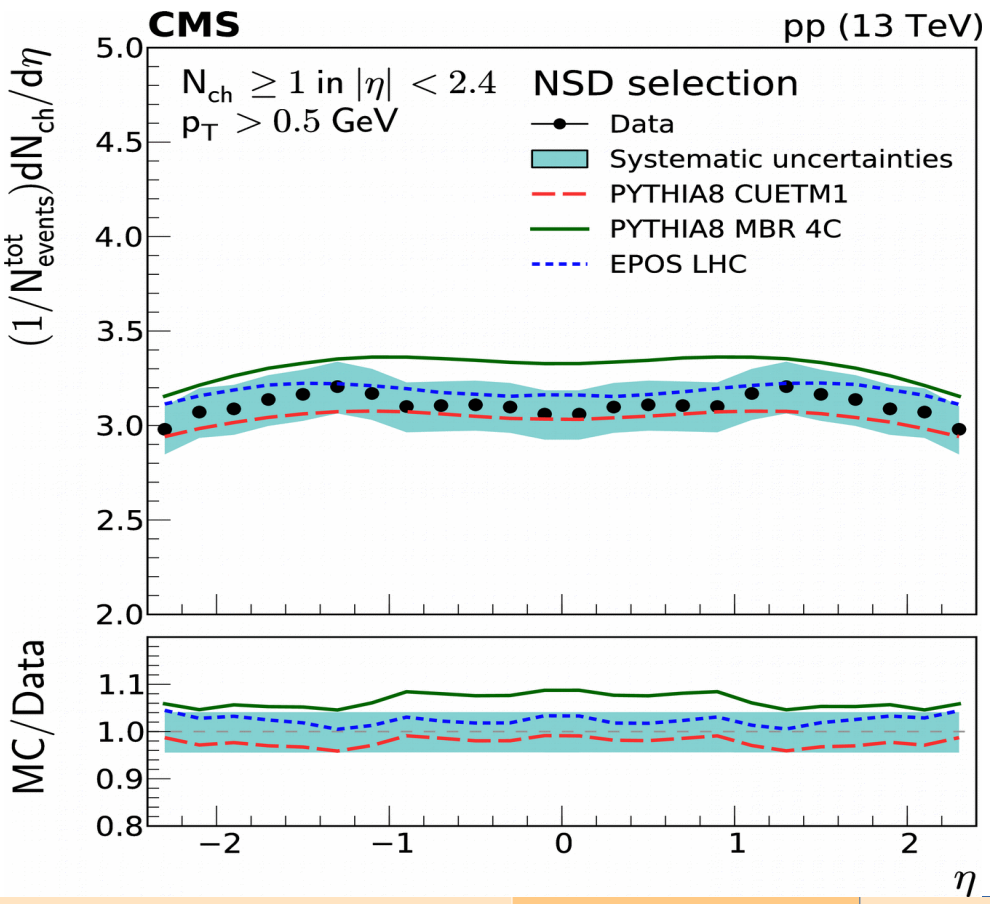

Charged-particle spectra in MB events at 13 TeV

- Integrated p_T spectrum of charged particles : sensitive to the transition b/w the non-perturbative and perturbative QCD regions

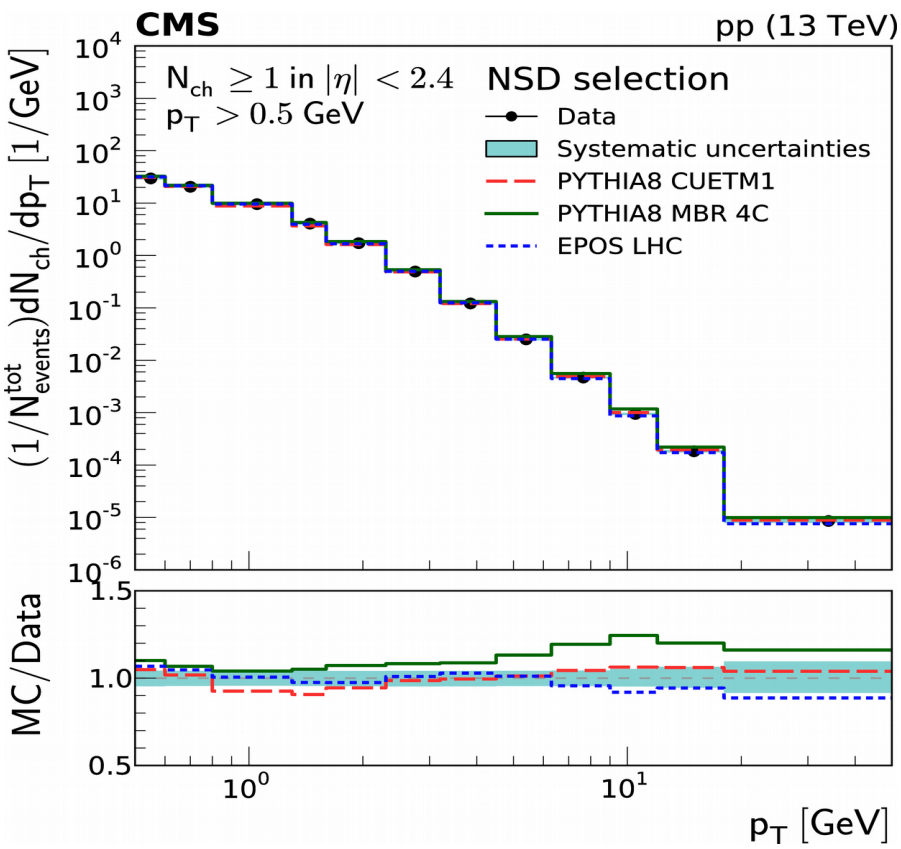

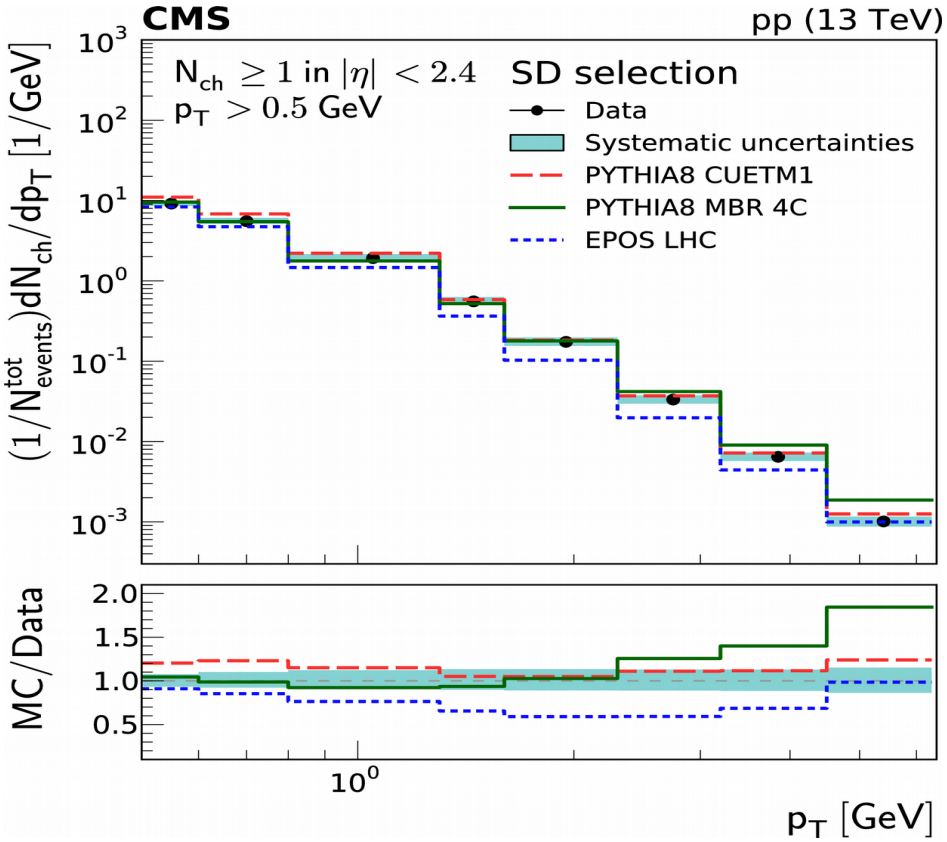

- NSD-enhanced events : EPOS LHC gives the best description, with small fluctuations
- SD-enhanced events : Low p_T region difficult to describe
- Transition between region dominated by particle production from MPI and hard scattering evident from fast change of slope

UE in top-quark pair production at 13 TeV

(Eur. Phys. J. C(79), 2, 123(2019)

- UE in $t\bar{t}$: - test "universality" assumptions at higher scales
  - direct probe of color reconnection (CR)
- Analysis performed using :

$$t\bar{t} \to (Wb)(Wb) \to (e\nu b)(\mu\nu b)$$

- All particle flow candidates with p_T > 900 MeV and |η| < 2.1 with track closest in z to PV

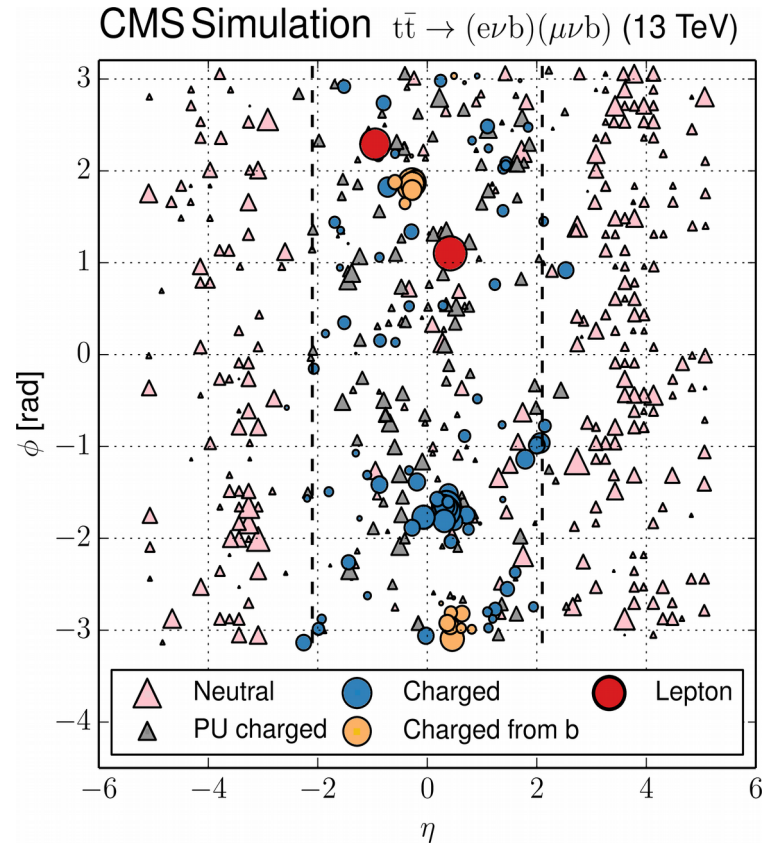

- Various observables are chosen to highlight the different features to which the tested models are sensitive :

- **Flux related observables**
  - charged particle multiplicity: N_{ch}
  - scalar sum of the p_T (or p_Z) of charged particles: $\Sigma p_T \ (or \ \Sigma p_Z)$
  - average p_T(or p_Z) per charged particle: $\overline{p_T} \ (or \ \overline{p_z})$
- **Event shape observables from the sphericity tensor**

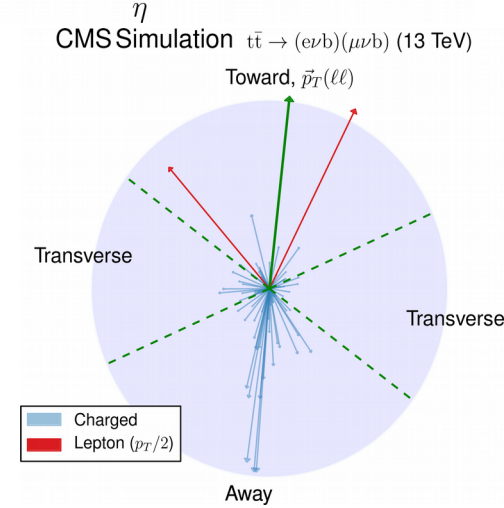

Results : Inclusive distributions

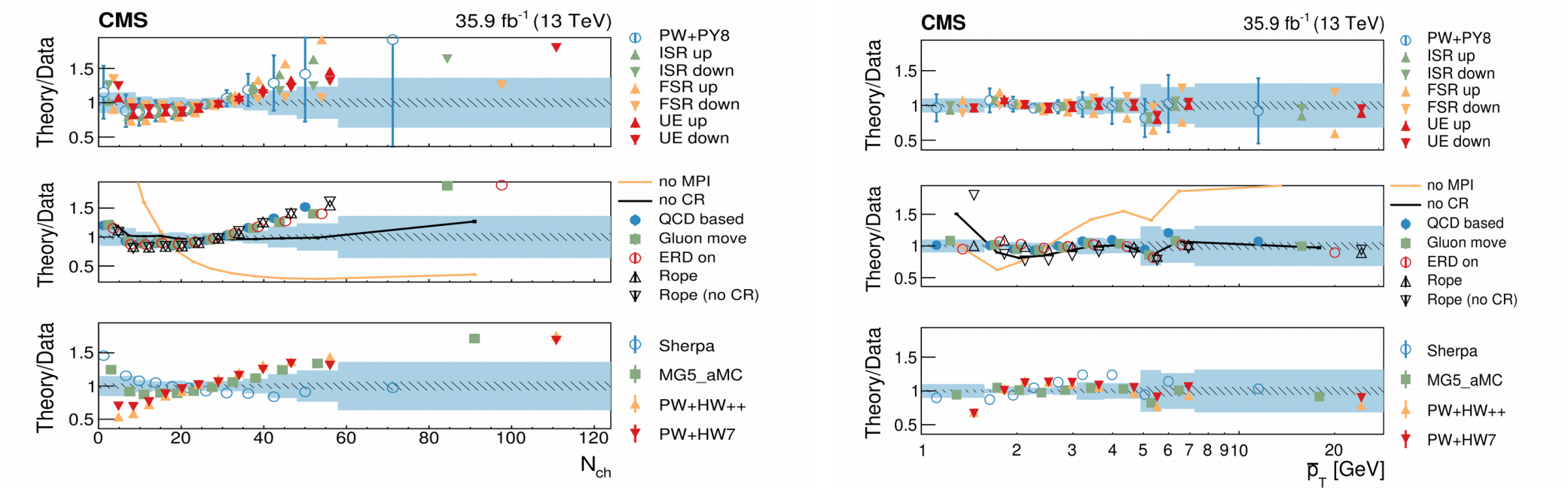

- **Negligible dependence on ME generator (PW+P8 vs aMC@NLO+P8)**
- **MPI contribution clear : switching off this component has a drastic effect in all variables**
- **CR effects are more subtle:**
  - CR needed to improve the accuracy for av. P_T < 3 GeV or av. P_Z < 5 GeV
- **In general, PW+P8 setup in agreement with data when total theory uncertainties taken into account:**
  - In most distributions, the variations of α_s^{FSR} leads to the most visible changes in the UE
- **While describing UE event shapes, the default settings of HERWIG++/7 tend to disagree in N_{ch}, av. p_T, av. p_Z. opposite behaviour observed in SHERPA**

Results : Sensitivity to the choice of α_s

- Sensitivity : tested by performing scan of χ^2 as a function of $\alpha_s^{ISR}(M_z)$ and $\alpha_s^{FSR}(M_z)$. No sensitivity observed for $\alpha_s^{ISR.}(M_z)$
- Most sensitive distribution : av. P_T

$p_T(\ell\ell)$ region	Inclusive	Away	Toward	Transverse
Best fit $\alpha_S^{FSR}(M_Z)$	0.120	0.119	0.116	0.119
68% CI	$[-0.006, +0.006]$	$[-0.011, +0.010]$	$[-0.013, +0.011]$	$[-0.006, +0.006]$
95% CI	$[-0.013, +0.011]$	$[-0.022, +0.019]$	$[-0.030, +0.021]$	$[-0.013, +0.012]$
μ_R/M_Z	2.3	2.4	2.9	2.4
68% CI	[1.7, 3.3]	[1.4, 4.9]	[1.6, 7.4]	[1.7, 3.5]

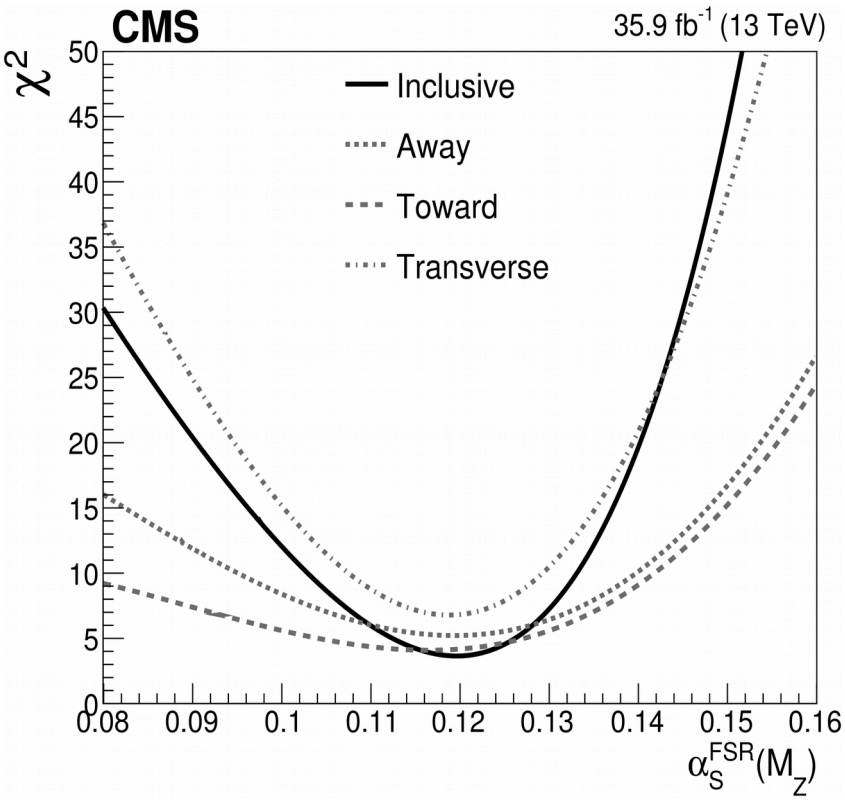

- Value of $\alpha_s^{FSR}(M_z) = 0.120 \pm 0.006$, significantly lower than one assumed in the MONASH tune, and the new CMS default tune CP5 uses $\alpha_s^{FSR)}(M_z) = \alpha_s^{ISR}(M_z) = 0.118$ (CMS PAS-GEN-17-001)
- Value obtained is compatible with one obtained from differential cross sections measured as function of av. p_T in different $|p_T(ll)|$ regions

Results could be used to improve the assessment of systematics in top quark analyses and contribute to test the universality of the UE hypothesis at higher energy and mass scales than the ones at which the UE models are usually tuned

The uncertainties of **$\alpha_s^{FSR}(M_z) = 0.120 \pm 0.006$** translate to a variation of the re-normalization scale by factor of $\sqrt{2}$ which is assumed variation in top quark measurement in CMS

Double Parton Scattering (DPS)

In general MPI is a softer contribution,
But .....Some MPIs can be hard → **Double Parton Scattering (DPS)**

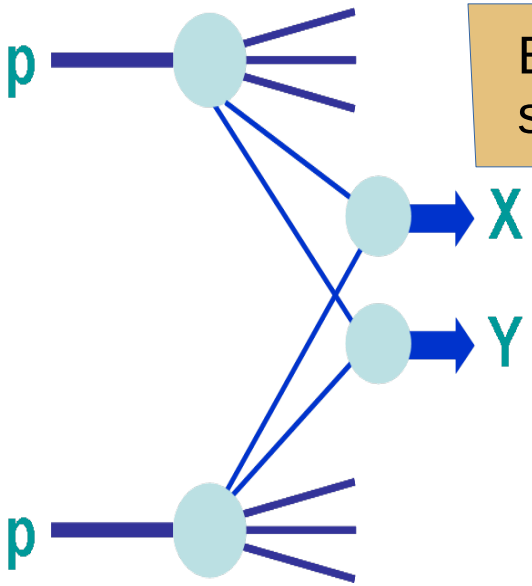

Events where two hard parton-parton interactions occur in single proton-proton collisions

DPS cross-section $\sigma_{eff} = \frac{m}{2} \cdot \frac{\sigma_X \cdot \sigma_Y}{\sigma^{DPS}_{X+Y}}$ $\begin{cases} m = 1 \text{ when } X = Y \\ m = 2 \text{ when } X \neq Y \end{cases}$

- Background for rare processes, e.g. Higgs , SUSY etc
- Provides information on transverse partonic distribution of hadrons

DPS

- W + 2 Jets (JHEP03(2014)032
- γ + 3 Jets (CMS PAS FSQ-12-017)
- 4 Jets (Phys.Rev.D89(2014)092010)
- 2bjet+2jet (Phys.Rev.D94(2016)112005
- Double J/Ψ (JHEP09(2014)094)
- Same-sign WW production

Why DPS using Same-Sign WW

- $\sigma^{DPS}_{W^\pm W^\pm} \approx \sigma^{SPS}_{W^\pm W^\pm}$ & a clean final state with leptonically decaying W bosons

DPS in same sign WW : Overall Strategy

select an inclusive region of phase space : minimal cuts for trigger and some QCD suppression

use most optimal objects possible to suppress backgrounds : especially on the lepton objects , (b-jet) vetos

train a BDT classifier against the most similar background -> WZ production

estimate backgrounds from data where possible (fakes, charge flips) : others from MC with validation where possible

make BDT classifier output distribution in eμ and μμ : perform constrained fit on whole distribution -> separate the charge for maximum sensitivity

- $p_T^{\ell_1}$ and $p_T^{\ell_2}$: transverse momenta of the two leptons;
- p_T^{miss};
- $\eta_1\eta_2$: product of η of the two leptons;
- $|\eta_1+\eta_2|$: absolute sum of η of the two leptons;
- $m_{T,(\ell_1,p_T^{miss})}$: transverse mass of the leading lepton and p_T^{miss};
- $m_{T,(\ell_1,\ell_2)}$: transverse mass of the two leptons;
- $|\Delta\phi_{(\ell_1,\ell_2)}|$: azimuthal angular separation between the leptons;
- $|\Delta\phi_{(\ell_2,p_T^{miss})}|$: azimuthal angular separation between the subleading lepton and p_T^{mi}
- $|\Delta\phi_{(\ell\ell,\ell_2)}|$: azimuthal angular separation between the dilepton system and the sub-leading lepton;
- $m_{T2}^{\ell\ell}$, the so-called "s-transverse mass" where the leptons serve as the two visible systems [48, 49].

The variable $m_{T2}^{\ell\ell}$ is defined as:

$$m_{T2}^{\ell\ell} = \min\left[\max\left(m_T^{(1)}, m_T^{(2)}\right)\right],$$

DPS in same sign WW at 13 TeV (PAS SMP-18-015)

CMS-PAS-SMP-18-015

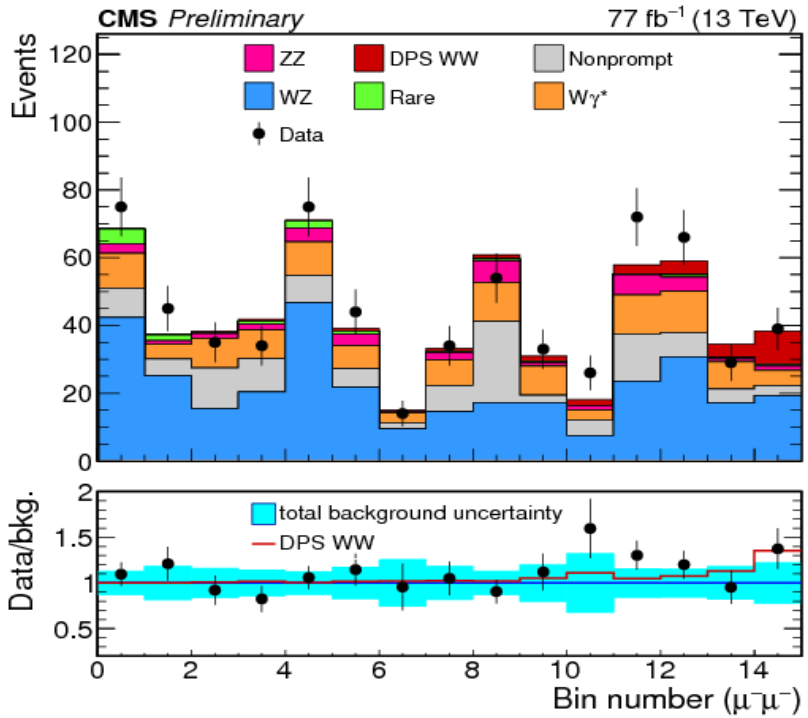

NEW

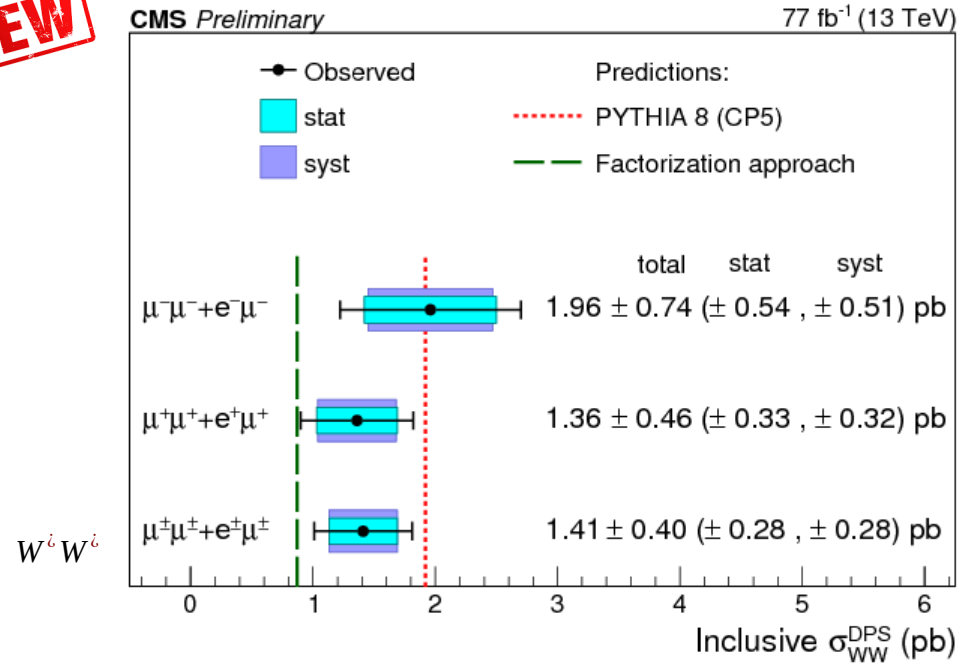

	obtained value	significance (standard deviations)
$\sigma_{DPS\,WW,exp}^{PYTHIA8}$	1.92 pb	5.4
$\sigma_{DPS\,WW,exp}^{factorized}$	0.87 pb	2.5
$\sigma_{DPS\,WW,obs}$	1.41± 0.28 (stat) ± 0.28 (syst) pb	3.9
σ_{eff}	$12.7^{+5.0}_{-2.9}$ mb	-

- A measurement of the double-parton scattering WW cross section is achieved for the first time, and a cross section of 1.41 ± 0.28 (stat) ± 0.28 (syst) pb is extracted with an observed significance of 3.9 standard deviations.
- σ_{eff} extracted from observed cross section is $12.7^{+5.0}_{-2.9}$ mb
- This result presents the first experimental evidence of the DPS WW process.

DPS in same sign WW at 8 and 13 TeV : Summary

- DPS measurements using same sign WW at 13 TeV using CMS detector are presented.
- An eventual observation of DPS process would permit to study the validity of the factorization approach, which is prevalent in current MC event generators.
- The DPS $W^{\pm}W^{\pm}$ process constitutes a background in searches for new physics at the LHC.
- 13 TeV result constitutes the first evidence of the DPS WW process.

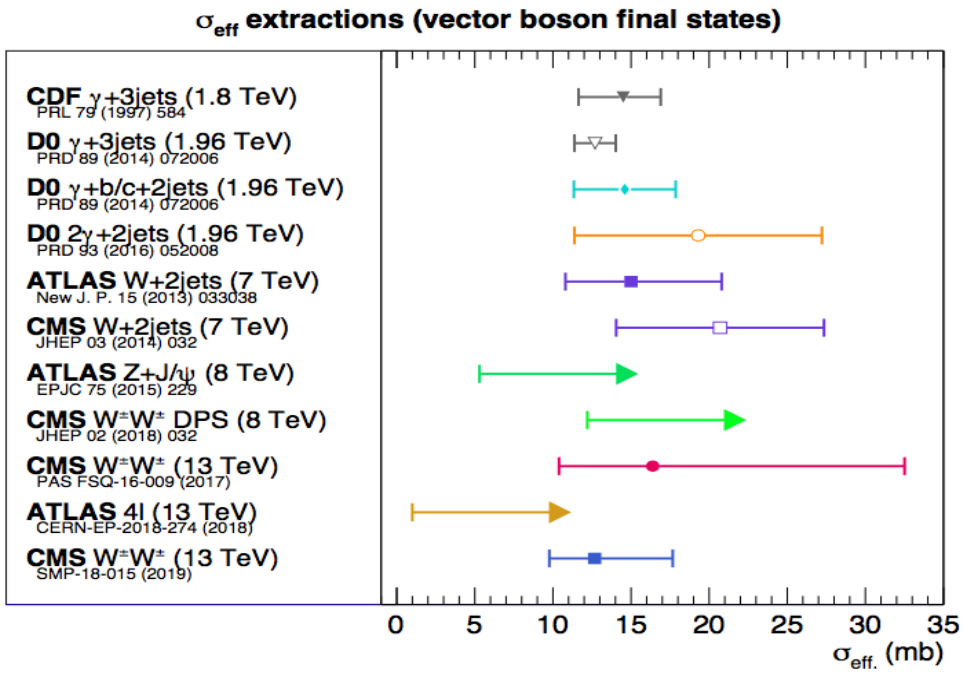

Extraction and validation of a new set of CMS PYTHIA8 tunes from underlying event measurements (arXiv:1903.12179)

- **A new set of tunes (CP1-5) for PYTHIA8 obtained with LO, NLO, NNLO versions of the NNPDF3.1 set**
  https://github.com/cms-sw/cmssw/tree/master/Configuration/Generator/python/MCTunes2017
- **Independent of the PDF used, new tunes describe well the UE at 1.96, 7 and 13 TeV.**
- **For the first time, it is seen that predictions based on higher-order PDF sets can give a reliable description of MB and UE, with a similar level of agreement from tunes with LO PDFs.**
- **The new tunes simultaneously describes the N_{ch} in diffractive and inelastic collisions.**
- **The new tunes and CUETP8M1 have a good description of forward N_{ch}, forward and very forward energy flow, and reasonable description of total energy spectrum in the very forward region.**
- **ME generators such as POWHEG and MG5_aMC with P8 with new tunes reproduce well the observables measured in multi-jets, DY and top-quark.**
- **CP5 now being used in 2017 and 2018 measurements/analyses**

Summary

- An overview of some representative soft and small-x QCD measurements has been presented.

- Long term goal : improve our picture of hadronic collisions, as well as its universality

- To get an insight into non-perturbative QCD as well as the behaviour of strong interactions at small-x.

- Understanding the non-perturbative regime:
  - High-precision and detailed studies provides input to improve phenomenological hadronic interaction models
  - Very advanced work in MC tuning
  - MPI a key element for a proper description of the final state
  - DPS as a tool for proton structure

- Great improvement of MC models, even if some inconsistency between data and MC still persists.

- Details on all presented results here :

http://cms-results.web.cern.ch/cms-results/public-results/publications/FSQ/index.html


Thank You


Backup
Ctrl

CMS Publications

- Measurement of inelastic pp cross section at 13 TeV, CMS FSQ-15-005 (JHEP07(2018)161)
- Charged-particle spectra in MB events at 13 TeV, CMS FSQ-16-011 (Eur. Phys. J. C (2018) 78: 697)
- Bose-Einstein Correlations (BEC) of Charged Hadrons, CMS PAS FSQ-15-009
- Measurement of inclusive very forward jet cross sections in proton-lead collisions at $\sqrt{s_{NN}}$ = 5.02 TeV, JHEP1905,043(2019)
- Measurement of the average very forward energy as a function of the track multiplicity at central rapidities in proton-proton collisions at 13 TeV (CMS PAS FSQ-18-001)
- Measurement of the underlying event in tt dilepton events at 13 TeV, (Eur. Phys. J. C(79), 2, 123(2019)
- Underlying Event Measurements with Leading Particles and Jets in proton proton collisions at $\sqrt{s}$= 13 TeV, CMS-PAS-FSQ-15-007.

CMS Publications

- **Measurement of the underlying event using the Drell-Yan process in proton-proton collisions at √s = 13 TeV, CMS FSQ-16-008, JHEP07(2018)032**
- **DPS in same sign WW at 8 TeV, CMS FSQ-16-005, JHEP02(2018)032**
- **Evidence for WW production from double-parton interactions in proton-proton collisions at at √s = 13 TeV, CMS-PAS-SMP-18-015**
- **Extraction and validation of a new set of CMS PYTHIA8 tunes from underlying event measurements (CMS PAS GEN-17-001)**

At leading order (LO) in the QCD coupling α_S, the pseudorapidity, η, and the p_T of a jet are related to the fraction x of the momentum of the parent nucleon that is carried by the incoming parton via

$$x \approx \frac{p_T}{\sqrt{s}} e^{\pm\eta}, \tag{1.1}$$

where $\sqrt{s}$ is the center-of-mass energy of the hadron-hadron collision. Forward jets with low p_T therefore probe the parton densities and their evolution at small (and large) x. The measurements presented in this paper, for jets with $p_T \geq 3\,\text{GeV}$ at very forward pseudorapidities $-6.6 < \eta < -5.2$, are thereby sensitive to fractional momenta down to $x \simeq 10^{-6}$. Collinear factorization and DGLAP have been shown to be successful for the description of processes involving large momentum exchanges and moderate fractional momenta carried by the interacting partons. However, in the low-x kinematic regime considered in this paper, this approach is expected to fail, whereas the Balitsky-Fadin-Kuraev-Lipatov (BFKL) equations [16–18], which evolve the parton densities as a function of $1/x$, should be better suited to describe forward jet production.

Both the DGLAP and BFKL equations are linear equations, i.e., they account for parton splitting and radiation, but not for parton recombination, processes. The BFKL and DGLAP equations predict a rapid rise of the gluon density towards small x, a result that has been experimentally confirmed by measurements at HERA [19]. This rise is mitigated when next-to-leading-order (NLO) corrections are taken into consideration. Despite this, the growth of the gluon density with decreasing x ultimately will result in a violation of unitarity (i.e., the cross section for parton scatterings will exceed the total inelastic hadronic cross section), and the linear evolution equations alone will not be sufficient to describe forward jet data. To solve this, it has been hypothesized [3] that at sufficiently small values of x, nonlinear gluon recombination processes will slow-down the uncontrolled growth of the PDFs. Such a parton "saturation" regime, characterized by a virtuality scale known as the saturation scale $Q_s(x)$, is described by the Balitsky-Kovchegov (BK) evolution equations [20, 21]. Saturation effects are expected to become important in the kinematic region where the gluon density, $xg(x, Q^2)$, times the transverse extent of the gluons, $\alpha_S(Q^2)/Q^2$, becomes equal to the transverse area of the hadron πR^2_{had} [22]:

$$\frac{\alpha_S(Q_s^2)}{Q_s^2} xg(x, Q_s^2) \approx \pi R^2_{\text{had}}. \tag{1.2}$$

In a heavy ion with number of nucleons A, the squared saturation scale Q_s^2 is expected to increase by a factor of $A^{1/3}$ with respect to that of a single nucleon, namely by approximately a factor of six for a lead nucleus. For $x \approx 10^{-6}$, the anticipated saturation scale in a lead nucleus is approximately $10\,\text{GeV}^2$ and, thereby, enhanced signals of gluon saturation are expected when colliding lead ions compared to protons at the LHC. Besides being a major research topic in its own right, parton saturation is also an important theoretical ingredient for describing the initial state of heavy ion collisions [23], and for understanding cosmic ray data [24].

The HIJING event generator models hard QCD interactions using the PYTHIA v5.7 [36] event generator, based on leading order collinear factorization and parton showering with DGLAP evolution. The Eichten-Hinchliffe-Lane-Quigg parameterization of the nucleon pdf is used [37]. The soft interactions are modeled with the Lund FRITIOF [38] and dual-parton [39] models. In addition, HIJING incorporates saturation effects via nuclear shadowing [22, 40, 41]. These shadowing corrections are obtained from a fit of the ratio of nucleus to proton sea quark structure functions at moderate x values ($x > 10^{-3}$), which are then extrapolated to lower x.

The EPOS-LHC program is an update of EPOS version 1.99 that has been specifically tuned to reproduce the first LHC p+p, p+Pb, and Pb+Pb measurements. This model uses a combination of soft pomeron exchange (as in Regge-Gribov theory [42, 43]) and a semihard contribution based on the convolution of a nonperturbative pre-evolution, a DGLAP-based hard evolution, and standard leading order QCD $2 \to 2$ cross sections [44]. The semihard contribution has been tuned to HERA structure function data and is recast as a hard pomeron amplitude. Saturation is modeled through pomeron-pomeron interactions and is implemented by modifying the x dependence of the pomeron amplitudes. In ref. [45], however, it is shown that this leads to too strong a suppression of the hard component, a shortcoming that will be remedied in an upcoming version of the model.

Similar to EPOS-LHC, the QGSJETII-04 model is based on the Regge-Gribov theory for the soft interactions and hard matrix elements convolved with DGLAP evolution for the hard scatterings. In this case, pomeron self-interactions result in saturation effects. The Cosmic Ray Monte Carlo CRMC package v1.5.6 [46] is used to generate the cross sections for the EPOS-LHC, HIJING, and QGSJETII-04 models.

In this paper, KATIE is used in a hybrid high-energy factorization approach where high-x partons in one incoming hadron are treated in the collinear framework, while low-x partons in the other incoming hadron are modeled using a TMD [47–50]. Such an approach is considered to be valid in configurations with very asymmetric fractional momenta, resulting, for example, in forward jet production. The TMDs are obtained from the Kutak-Sapeta (KS) framework [51], combined with linear (BFKL) or nonlinear (BK) evolution with running coupling, respectively. The strength of the nonlinear term can be varied; here, a default strength of 75% is used, with a variation of ±25% to reflect the sensitivity to nonlinear evolution. The parton density used in the collinear framework is the CTEQ10 NLO set [52]. The KATIE program is used to calculate leading order hard scattering matrix elements for the $2 \to 1$ process ($g^*q \to q$ or $g^*g \to g$) with incoming offshell gluons. The subsequent hadronization is modeled using CASCADE v2.4.13 [53]. A more in-depth description of the predictions that are included in the present paper can be found in ref. [54].

The AAMQS predictions [24] for the forward jet spectra are also obtained using hybrid factorization. At the parton level, the AAMQS model generates quarks and gluons from $gq \to q$ and $gg \to g$ hard processes, along with initial- and final-state radiation based on DGLAP evolution. The TMD is related to a dipole scattering amplitude in coordinate space via a Fourier transform and, in this paper, an implementation based on the McLerran-Venugopalan (MV) model [55–57] is used to derive the dipole scattering amplitude within the color glass condensate framework [20, 21, 58–63]. In this framework the hard partons act as color sources for a classical non-Abelian background field, which is formed by numerous soft gluons. The AAMQS calculations are performed at leading order in α_S. The evolution of the TMD is performed using the BK equation with running coupling strength. For the collinear PDFs the CTEQ6 LO set was used [64]. Multiple parton interactions are included

Measurement of inelastic pp cross section at 13 TeV (JHEP07(2018)161)

- **Analysis Strategy**
  Count events with an energy deposit above threshold

no. of events Above threshold → Data driven Correction for Noise and PU

$$\sigma = \frac{N_{\text{int}}(1 - b_\xi)}{\epsilon_\xi \mathcal{L}}$$

Integrated luminosity

Correction to particle level (efficiency & contamination) From MC simulation

Motivation:

- Input to improve phenomenological hadronic interaction models
- Important basic QCD measurement : crucial to model pile-up
- Challenging to measure precisely:
  - required good calibration of luminosity
  - extrapolation leads to significant model dependence

Two different event selections were chosen to have two cross-section measurements within Different acceptance

At least one HF tower above a threshold of 5 GeV (**HF OR**)	At least one HF or CASTOR tower above a threshold of 5 GeV (**HF OR CASTOR**)

Cross section results

- Fully Corrected cross section HF OR:

$$\sigma(\xi > 10^{-6}) = 67.5 \pm 0.8\,(\text{syst}) \pm 1.6\,(\text{lumi})\,\text{mb},$$

Consistent with a previous measurement in the same phase space

- Fully Corrected cross section HF OR CASTOR:

$$\sigma(\xi_X > 10^{-7}\,\text{or}\,\xi_Y > 10^{-6}) = 68.6 \pm 0.5\,(\text{syst}) \pm 1.6\,(\text{lumi})\,\text{mb},$$

Smaller than those predicted by the majority of models for hadron-hadron scattering, as observed in 7 TeV

Whereas same models describes the measurements of total inelastic cross section at 13 TeV

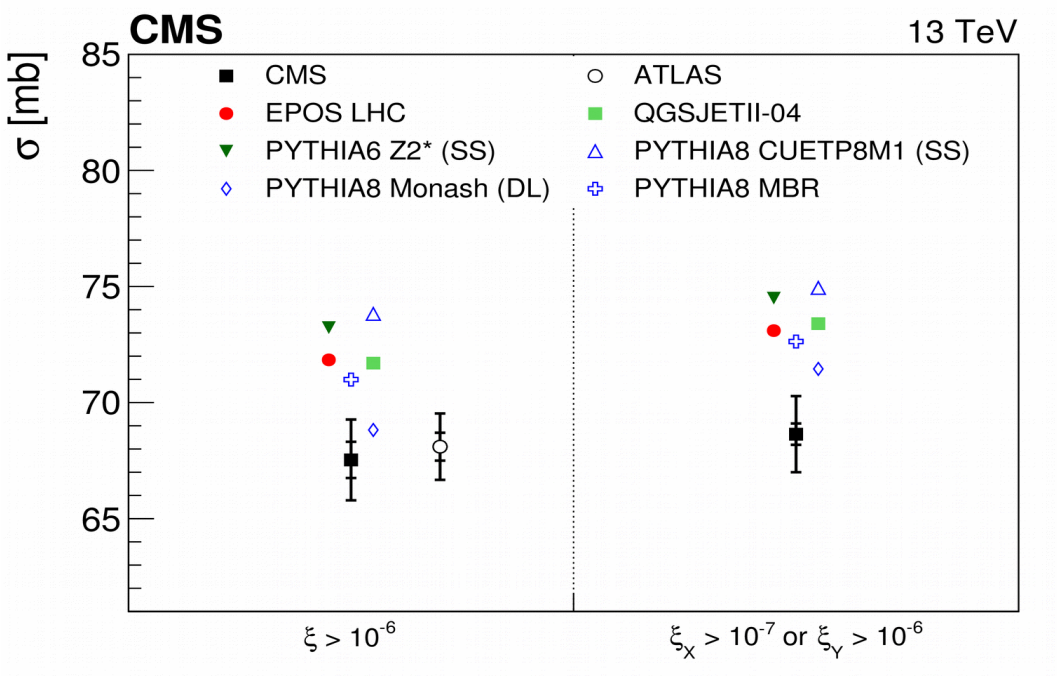

ATLAS Results:

$\sigma(\xi > 10^{-6}) = 68.1 \pm 0.6\,(\text{syst}) \pm 1.3\,(\text{lumi})\,\text{mb}$

10.1103/PhysRevLett.117.182002

TOTEM Results:

$$\sigma_{\text{inel}} = (79.5 \pm 1.8)\ \text{mb}.$$

arXiv:1712.06153

Bose-Einstein Correlations (BEC) of Charged Hadrons (PAS FSQ-15-009)

- BEC : Probes the size and shape of the particle emitting region in high-energy collisions
- Correlation function extracted using double ratios and two data-driven (cluster subtraction & hybrid cluster subtraction) methods
- Homogeneity length (R_{inv}) studied as a function of particle multiplicity (N_{tracks}) at the particle level, average pair transverse momentum (k_T) and mass (m_T)

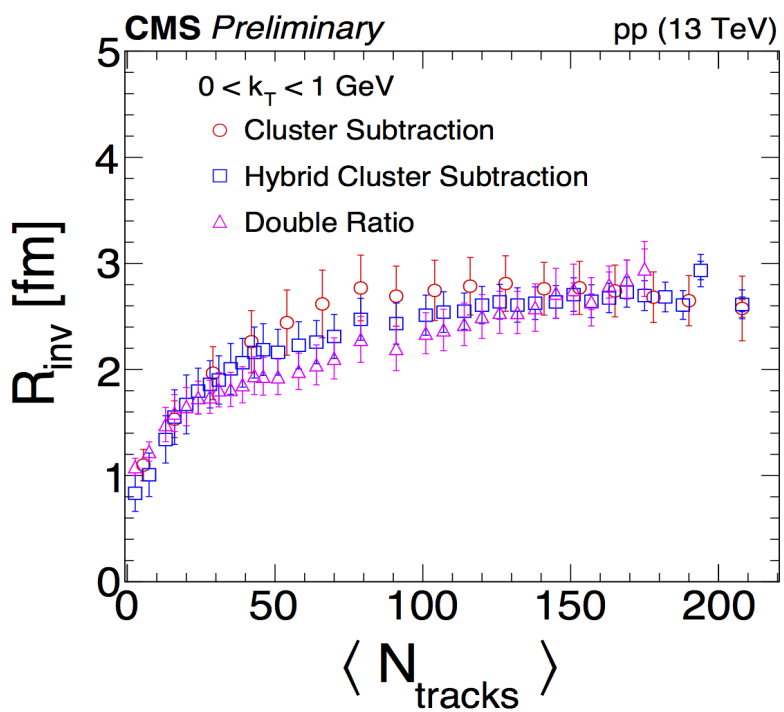

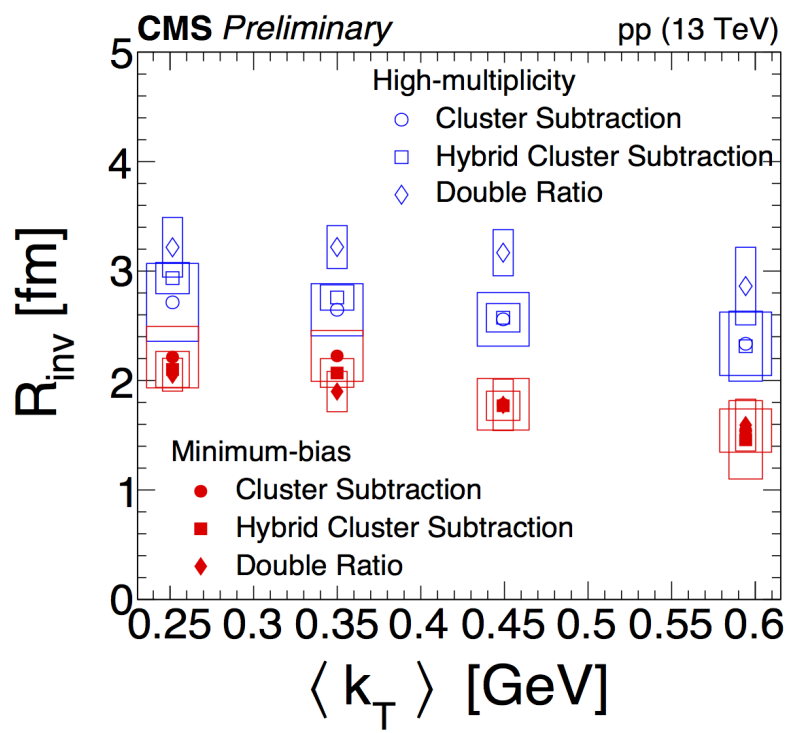

- R_{inv} increases with $< N_{tracks} >$ and saturates at higher values
- R_{inv} decreases with increasing k_T ⟶ Emitting source was expanding prior to decoupling

Results: m_T Dependence

Hydrodynamic Models :

- Intercept connected with the geometrical size of the source (at freeze-out)
- Slope connected to the flow component, bigger slope (bigger flow) for lower multiplicities

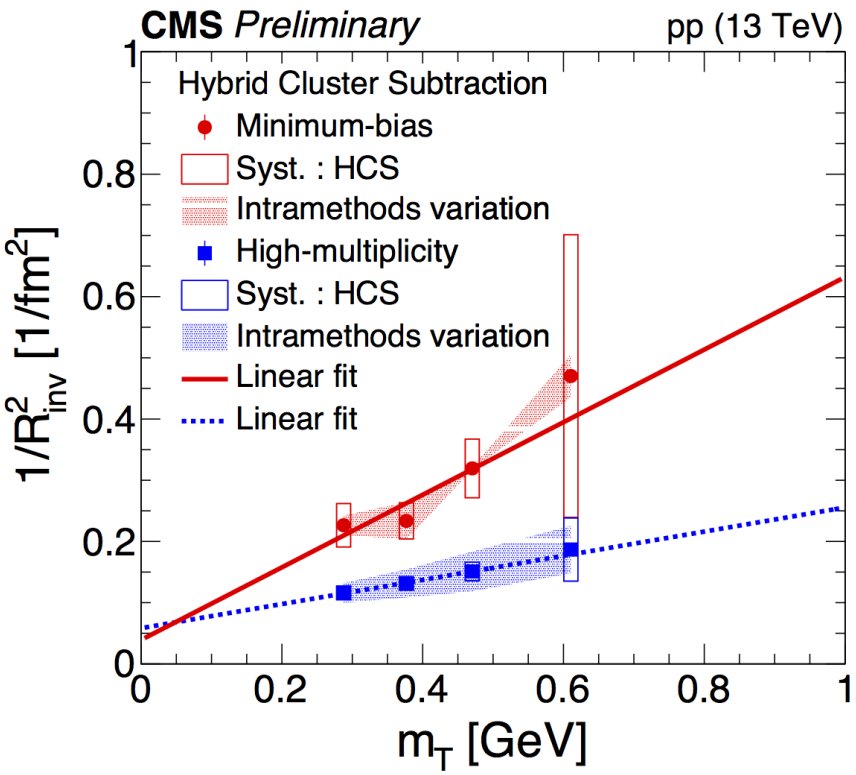

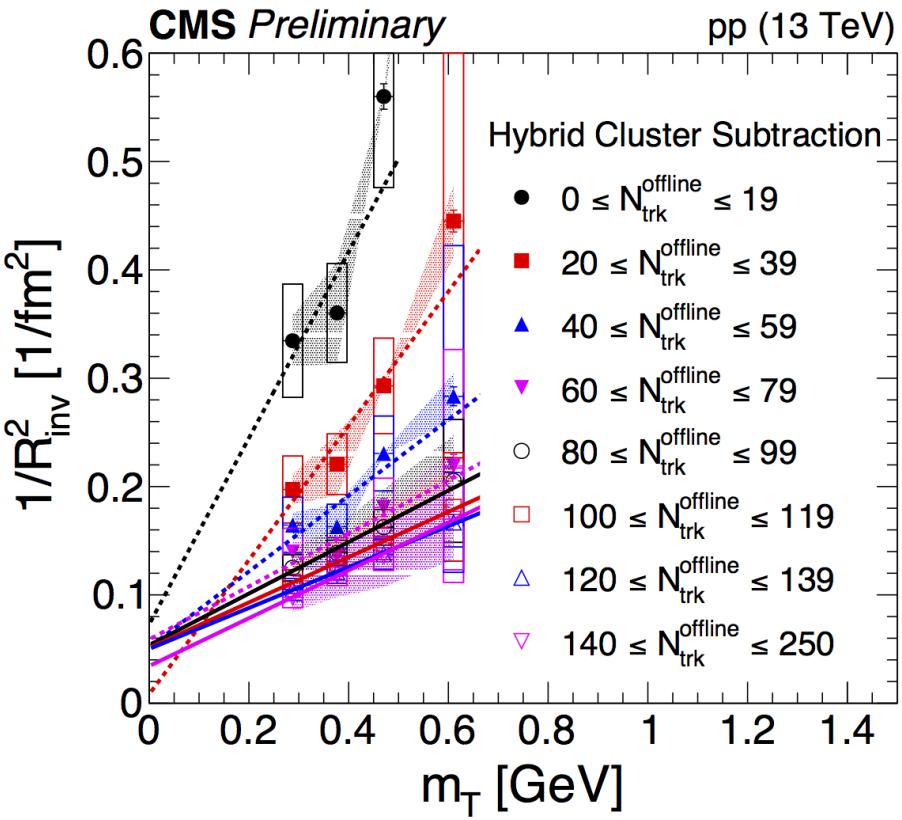

- Expansion in the low multiplicity region is faster than in the high multiplicity region
- Collective flow decreases with increasing multiplicity and saturates at around 80

Underlying Event (UE) Using DY Process (JHEP07(2018)032)

Underlying event using Drell-Yan process with muonic final state:

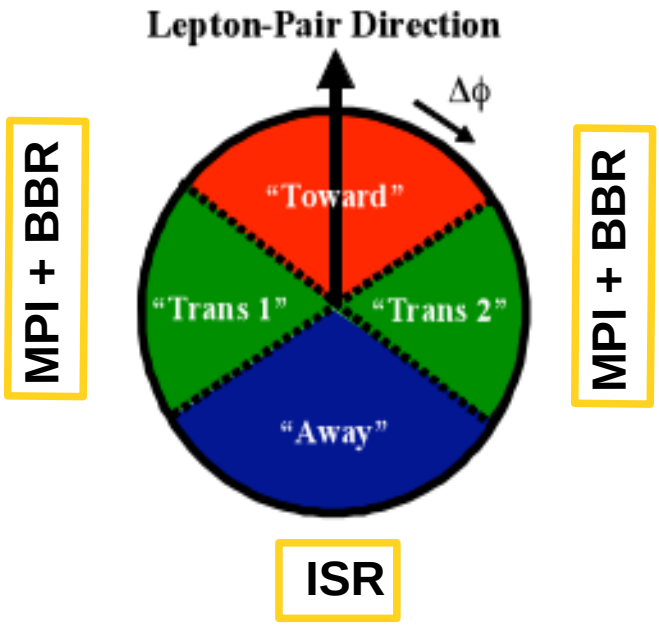

- 2 muons from Z leptonic decay with $p_T > 10$ & 20 GeV, $|\eta| < 2.4$ & $81 < M_{\mu\mu} < 101$ GeV
- charged particles with $p_T > 0.5$ GeV & $|\eta| < 2$ in the towards, transverse and away region.
- No Final-State Radiation → more direct access to MPI and Initial-State Radiation
- Test the UE process universality and universality of the tunes interfaced with different event generators.

UE observable:

Avg charged particle multiplicity density:

$\langle N_{ch} \rangle / [\Delta\eta\Delta(\Delta\varphi)]$,

Average Scalar sum of transverse momenta

$\langle \Sigma p_T \rangle / [\Delta\eta\Delta(\Delta\varphi)]$

JHEP07(2018)032

These observables are studied as a function of $p_T^{\mu\mu}$, in away, towards and transverse regions.

UE in DY – avg particle density vs dimuon p_T

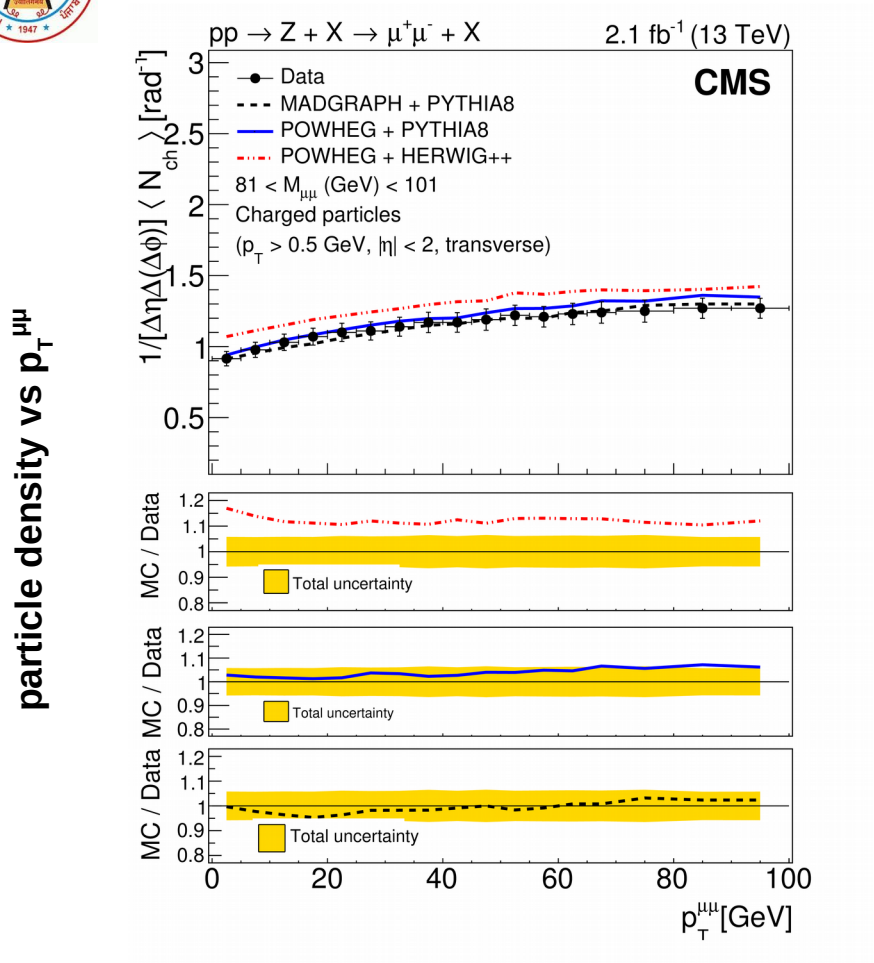

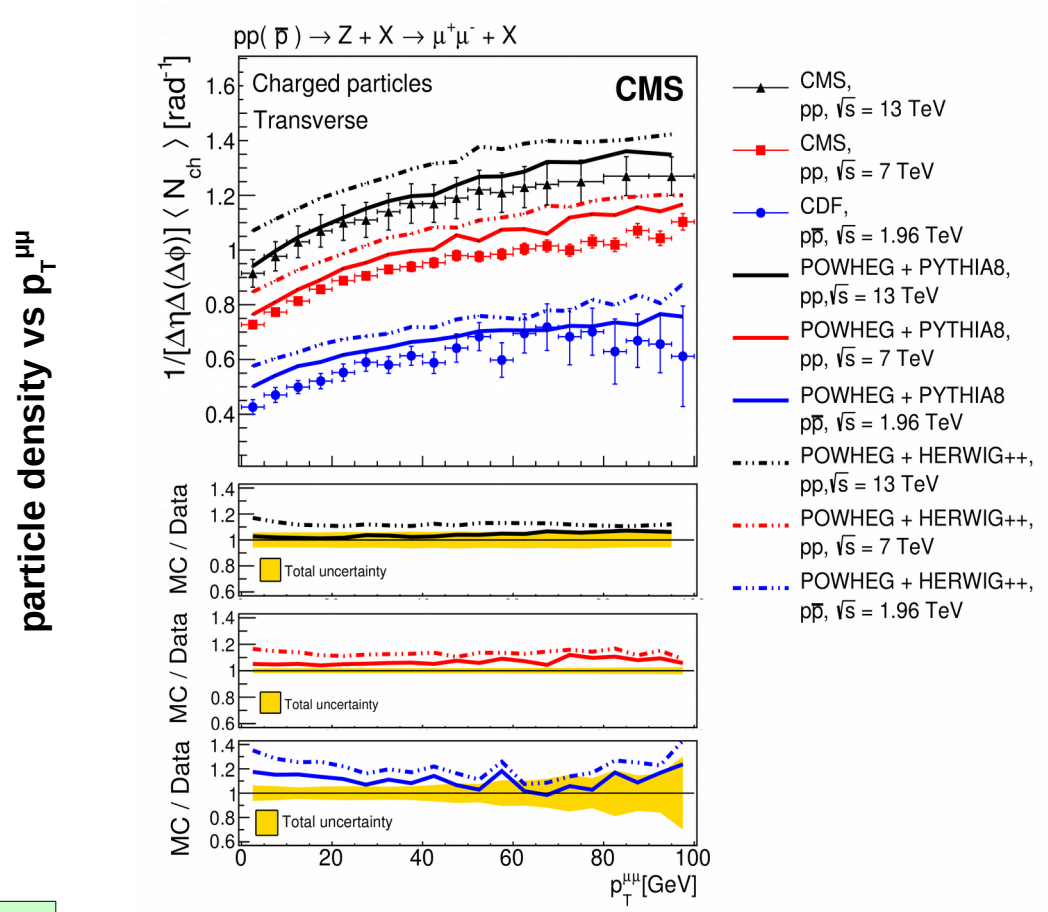

- POWHEG + HERWIG++ EE5c: overestimates UE activity by 10-15% in all regions
- POWHEG + PHYTHIA8 CUETP8M1: describes the data within 5%
- MADGRAPH + PYTHIA8 CUETP8M1: gives the best description

- 1.96 TeV → 7 TeV → 13 TeV:
- POWHEG + HERWIG++ EE5c: overestimates data by 40 to 10%.
- POWHEG + PHYTHIA 8 CUETP8M1: describes data within 10 to 5%.

UE in DY : activity at different energies

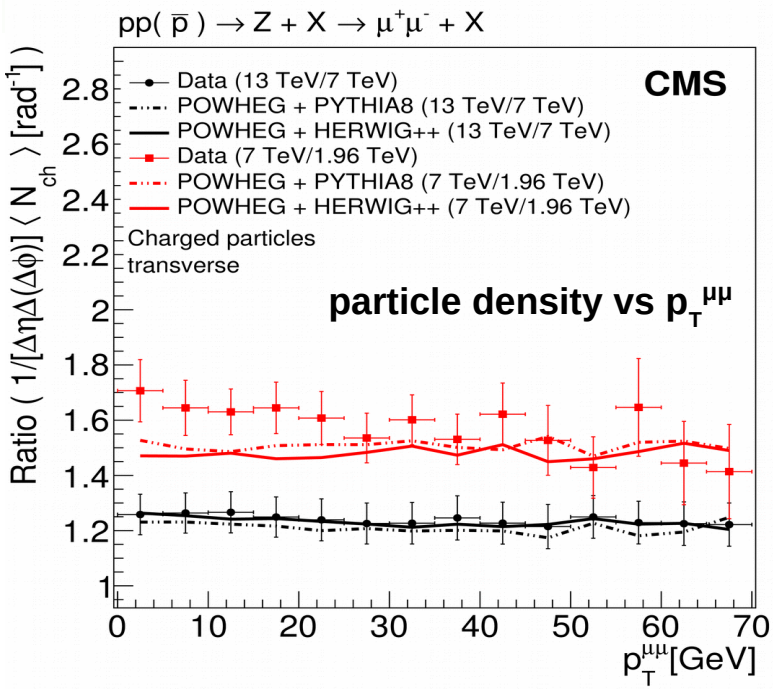

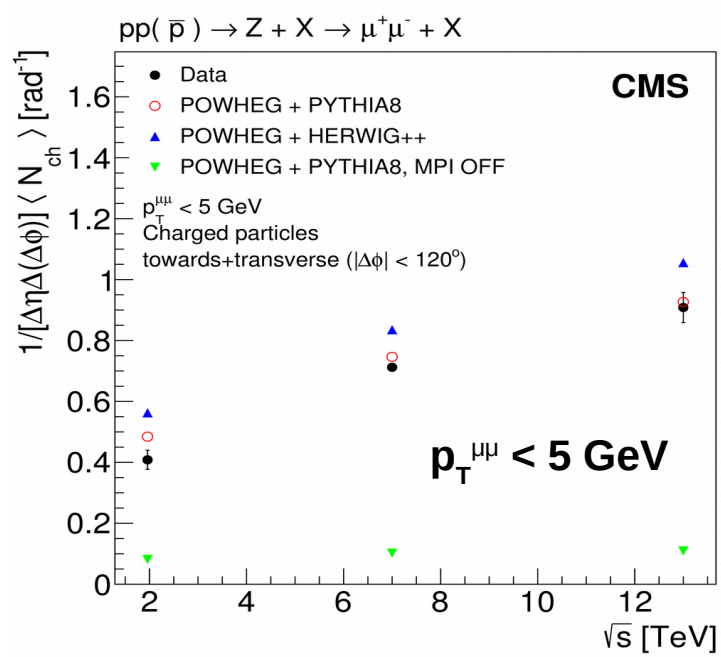

- To quantify increase in UE : ratios are calulated $(UE)_{13(7)\ TeV}$ / $(UE\ activity)_{7(1.96)\ TeV}$ for both simulation and data.
- 25-30% rise from 7 to 13 TeV , models in good agreement.
- 60-80% rise from 1.96 TeV to 7 TeV, models predict lower increase particularly at lower p_T

- At low dimuon p_T : underlying event activity dominated by MPI contributions.
- Average particle and energy density for dimuon p_T as a function of CM energy in the combined towards and transverse region.

- POWHEG + PYTHIA8 Without MPI : contribution from radiation very small.
- Increase of MPI activity well reproduced by POWHEG + PYTHIA8.
- Overestimated by POWHEG + HERWIG++.

Physics Objectives:

Scattering

- Elastic and diffractive scattering represent ~50% of the total cross-section
- Leading proton scattering within the beam pipe detected by the Roman Pots

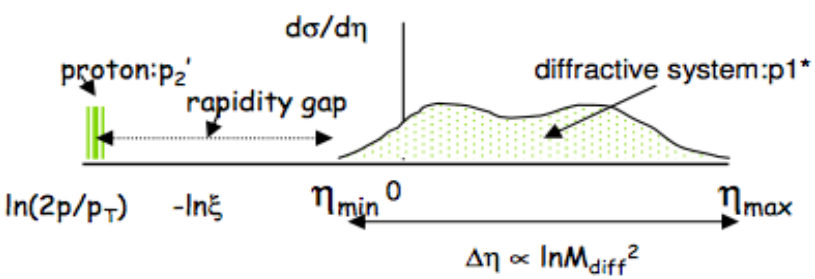

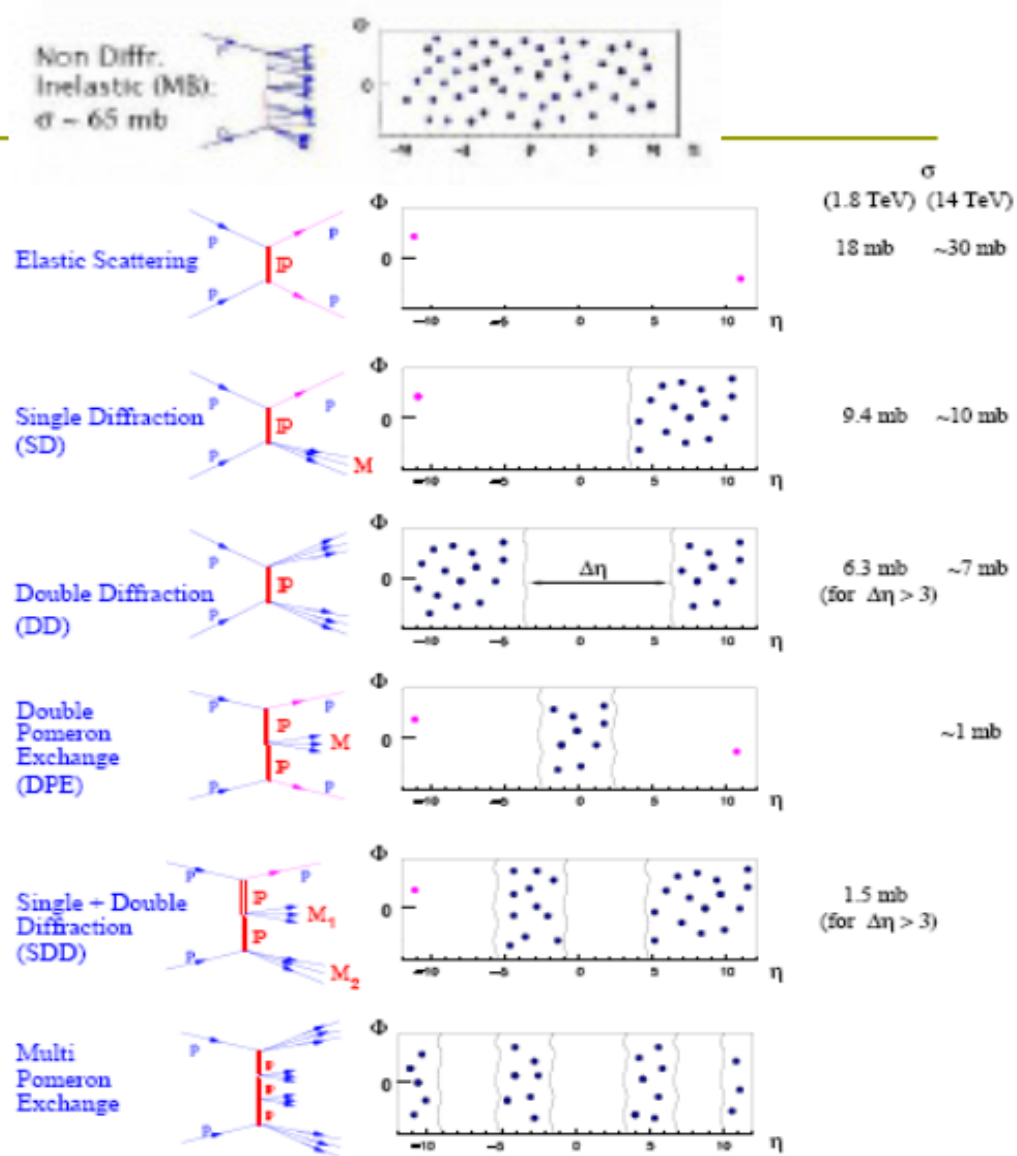

Inelastic Scattering

Non-diffractive

Colour exchange

Diffractive

Colourless exchange with vacuum quantum numbers

Incident hadrons acquire colour and break apart

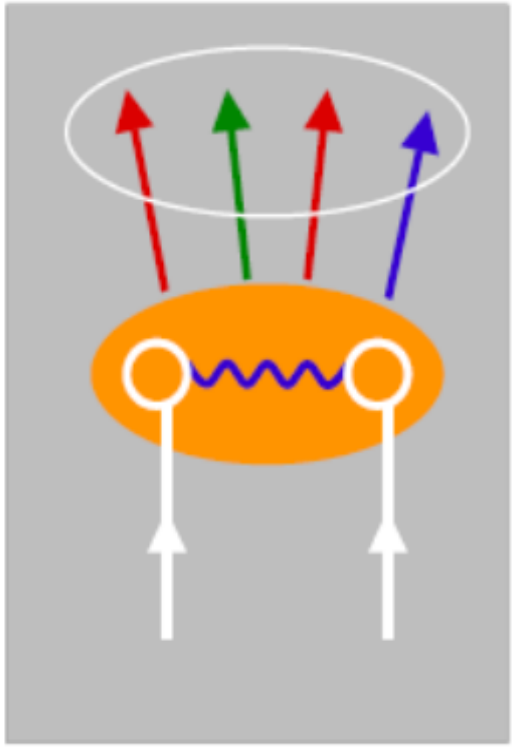

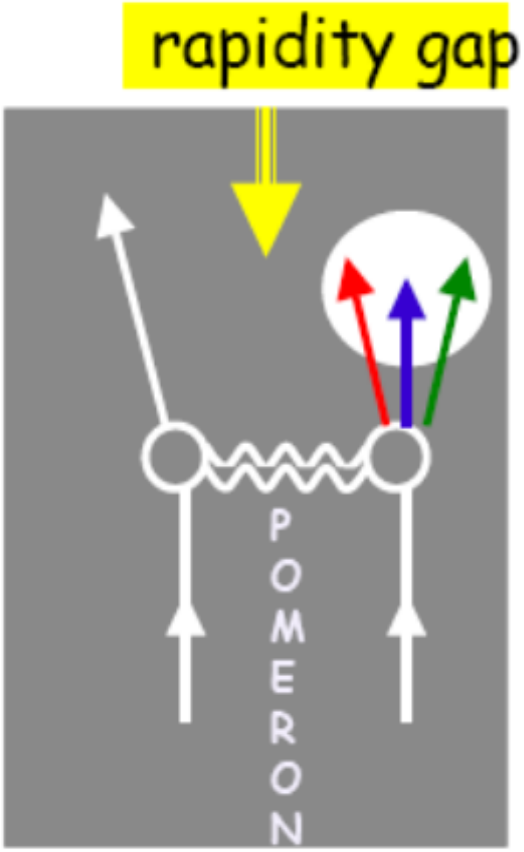

Incident hadrons retain their quantum numbers remaining colourless

Detector Overview:

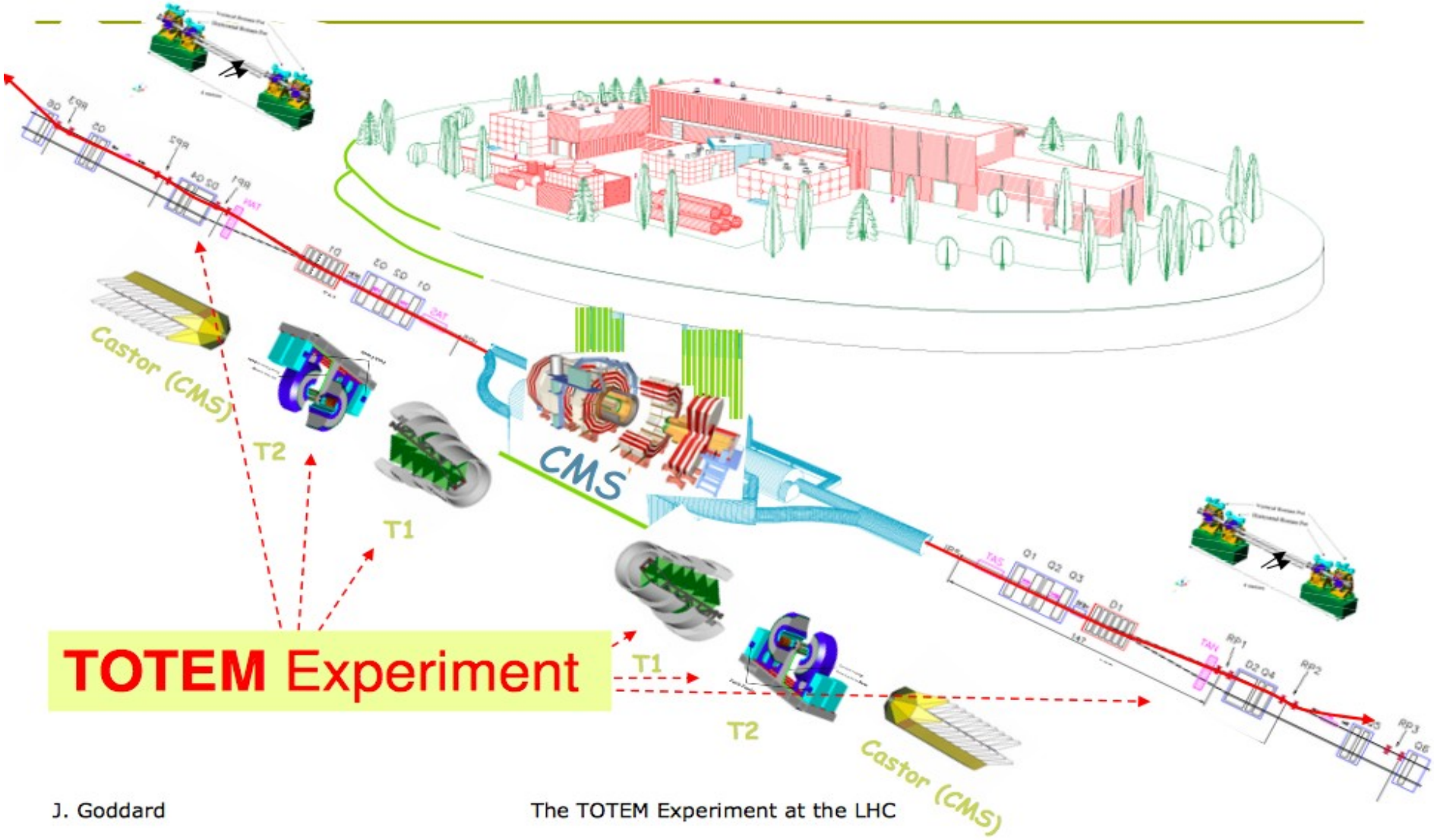

HF and CASTOR calorimeters

- HF:
  - 18 iron φ wedges
  - long+short quartz fibres
  - at both sides of CMS: HF- and HF+
  - Nominal acceptance: 3.0 < |η| < 5.2
  - Energy scale known to ±10%

  ➔ 2 lowest rings not used
  (one lies in shadow of HE, second too noisy)
  ➔ actual acceptance: **3.152 < |η| < 5.205**

- CASTOR:
  - 16 φ sectors, 14 z-modules
  - tungsten / quartz plates
  - only on minus side of CMS
  - Acceptance: **-6.6 < η < -5.2**
  - Energy scale known to ±15%
  - Alignment known to ±2 mm
  - **only present during B = 0 T data taking**

HF φ-wedge

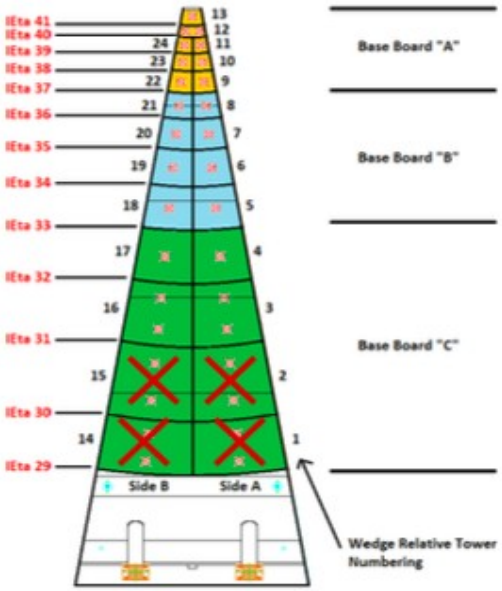

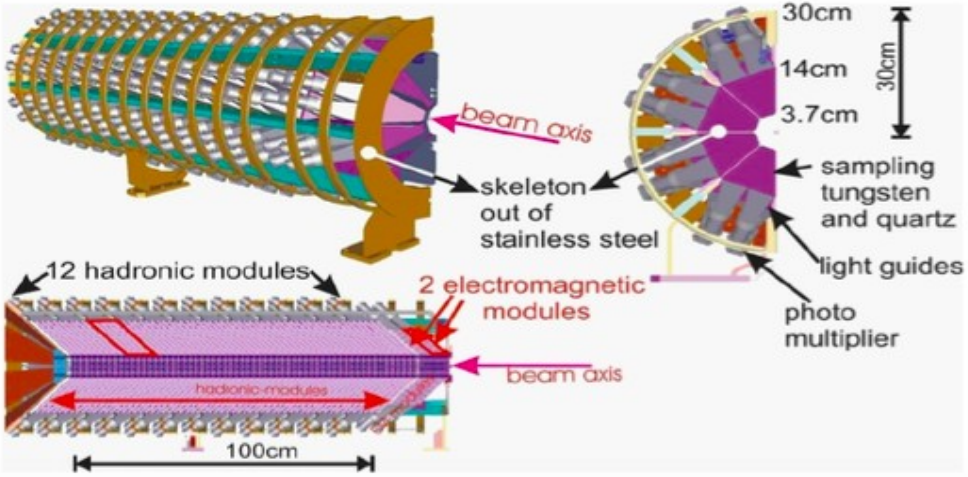

Diffraction

$$\sigma_{tot} = \sigma_{el} + \sigma_{ine}$$
$$= \sigma_{el} + (\sigma_{SD} + \sigma_{DD} + \sigma_{CD} + \sigma_{ND})$$

Described by the exchange of a color-neutral object

Pomeron

Soft and Hard diffraction

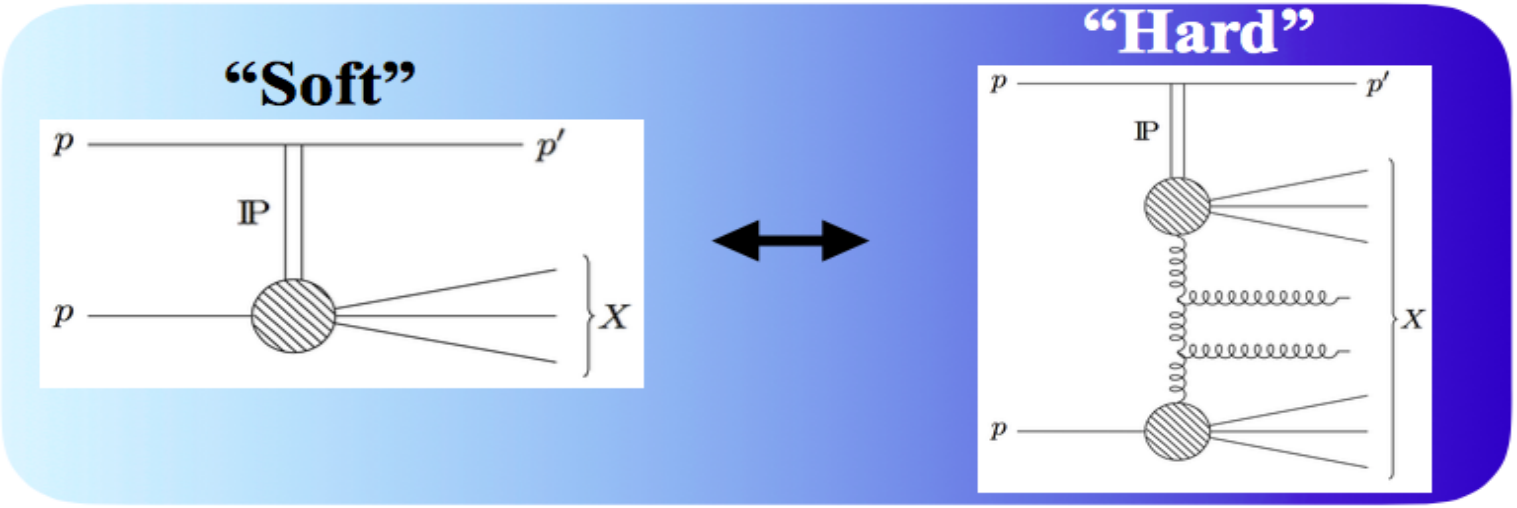

Diffraction

Described by the exchange of a color-neutral object

Pomeron

Pythia8 predictions at 13TeV

			σ_{NSD}		
σ_{tot}	σ_{el}	σ_{SD}	σ_{DD}	σ_{CD}	σ_{ND}
100mb	25mb	15mb	10mb	~1mb	50mb
		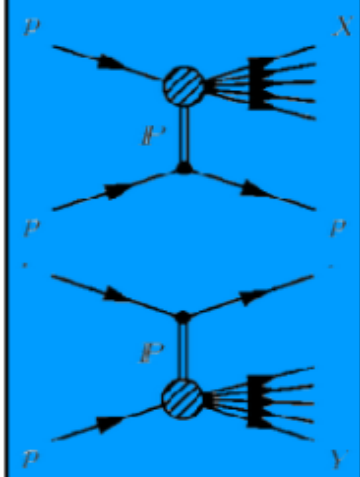	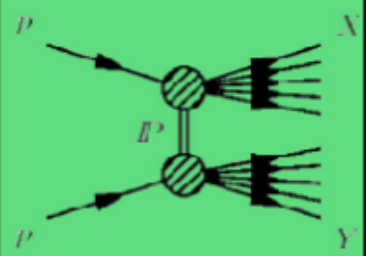	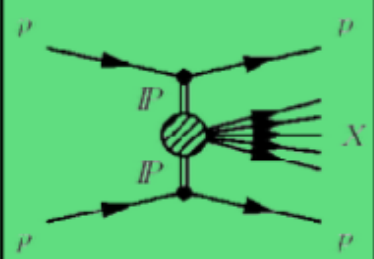	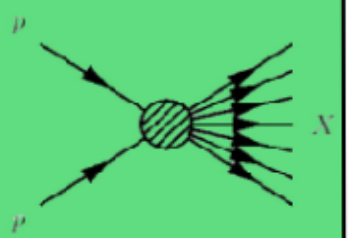

Model comparison

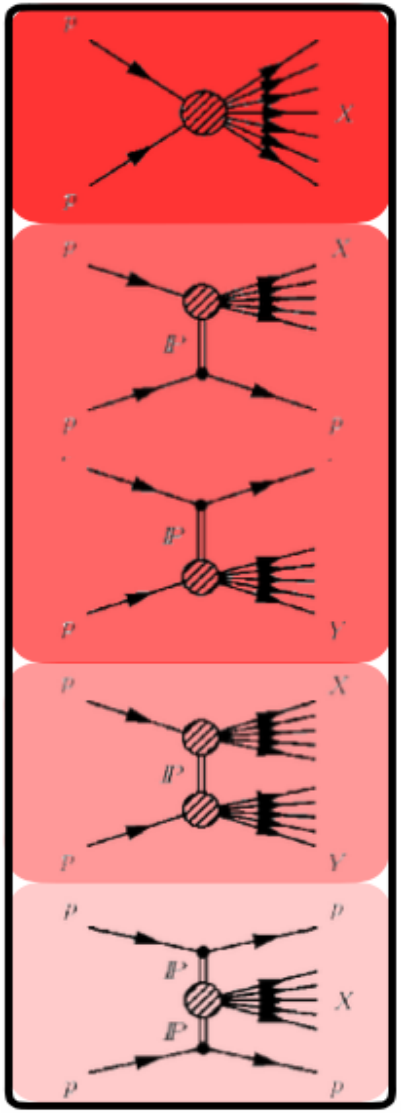

Inelastic enhanced Sample

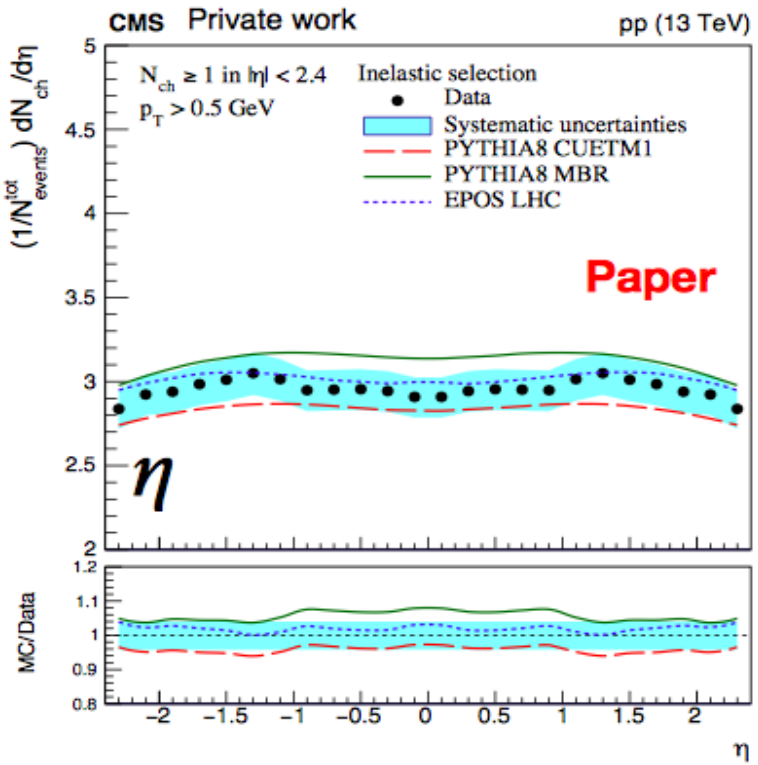

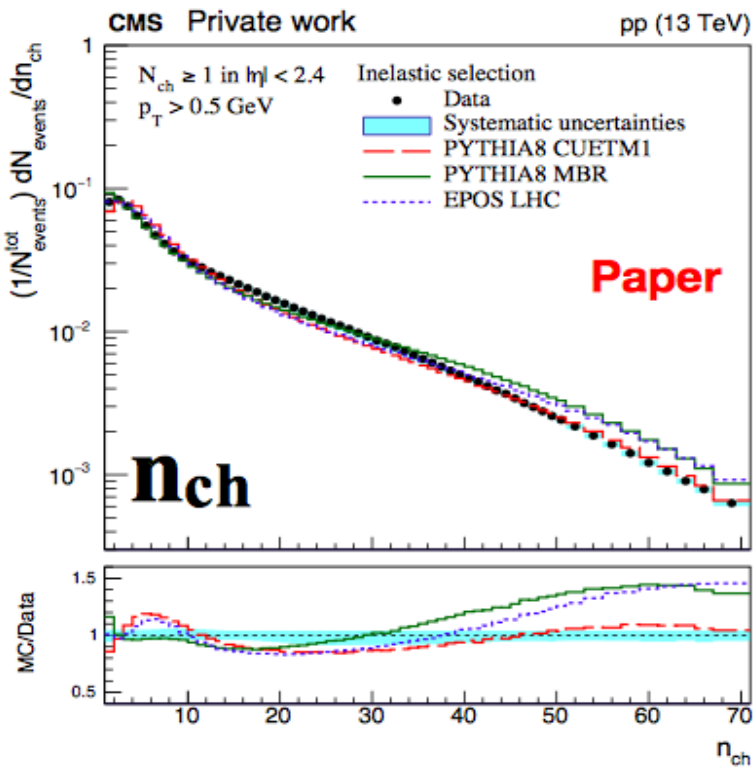

- Similar **shape** predictions
- Different **density** predictions
- Over estimation at low and high multiplicities

38

Model comparison

SD enhanced Sample

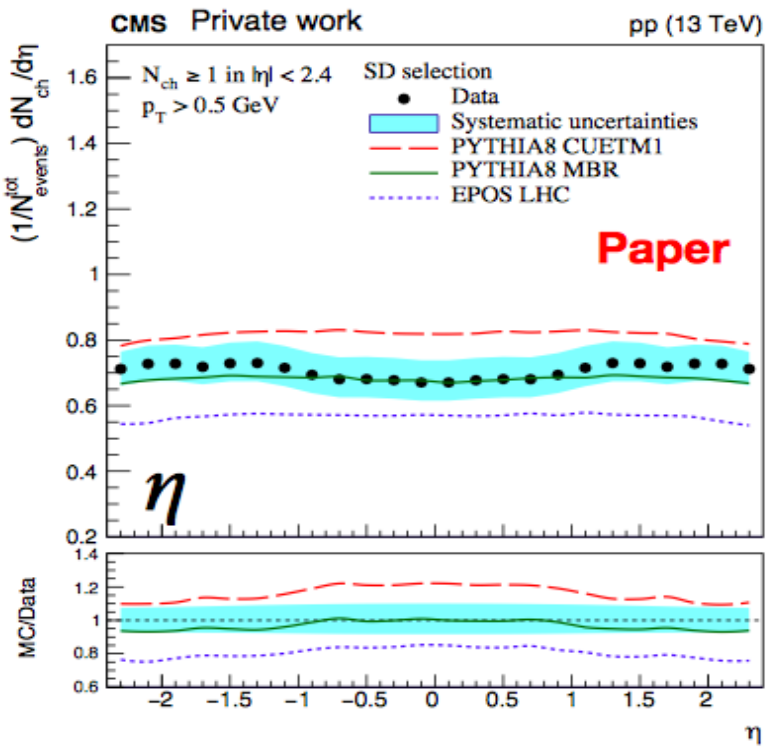

SD-One-Side enhanced sample

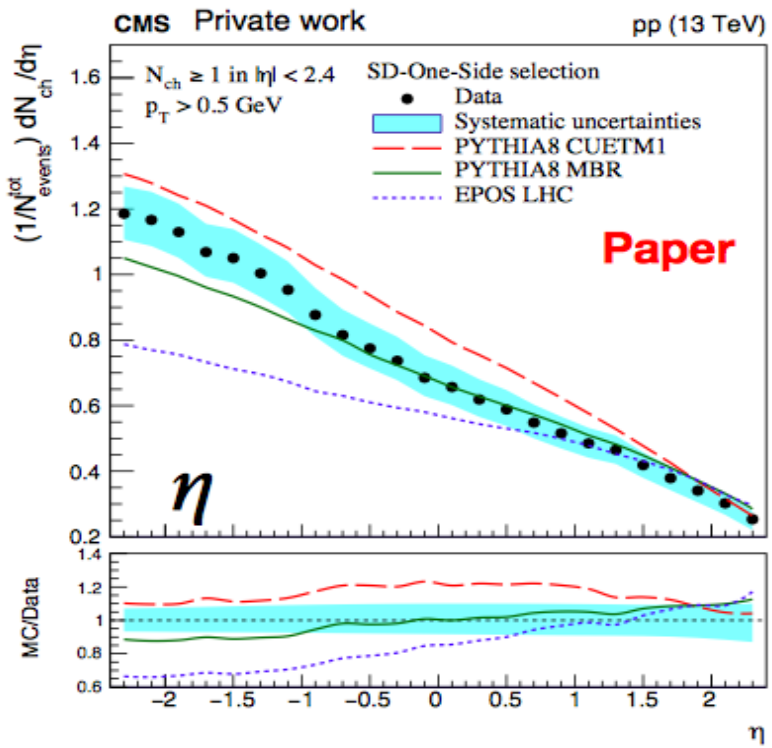

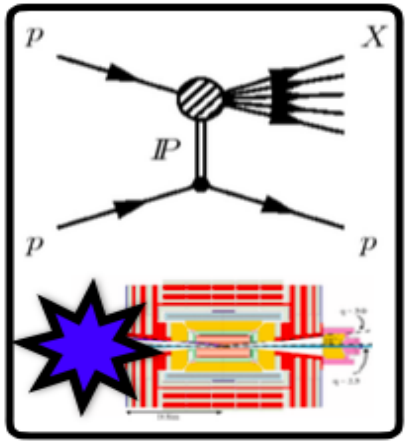

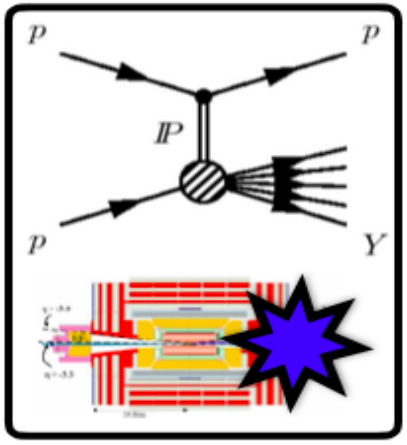

- **MBR** tuned to **diffractive** distributions
- Scattered proton side **well** described
- Diffractive system **not well** described

39

Model comparison

Non-SD enhanced Sample

SD enhanced Sample

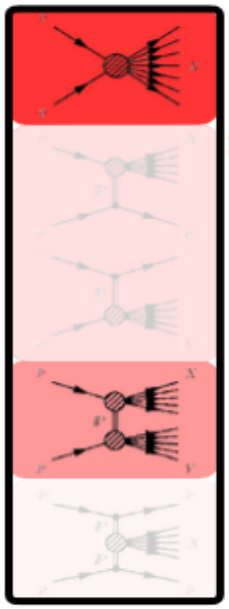

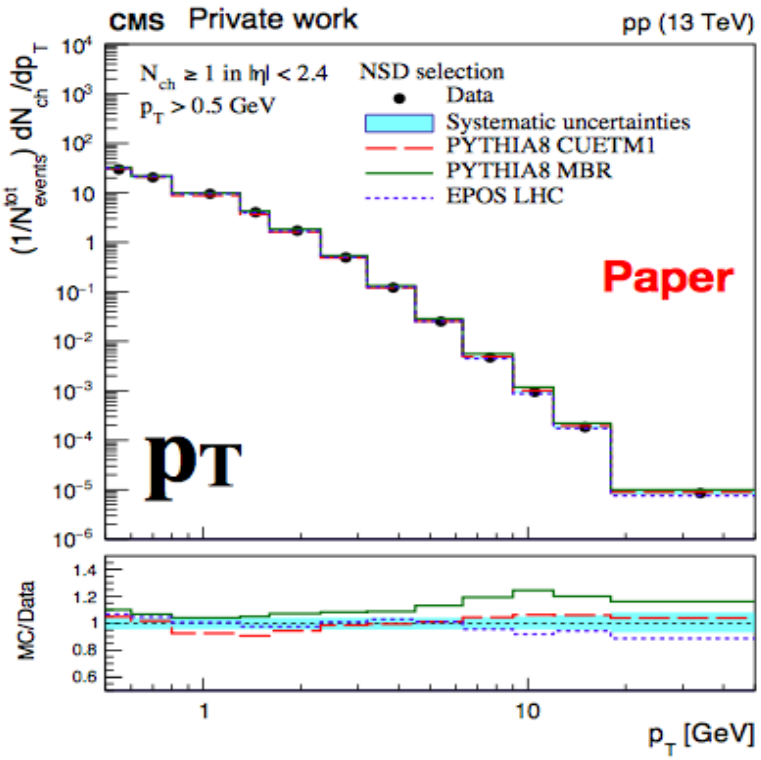

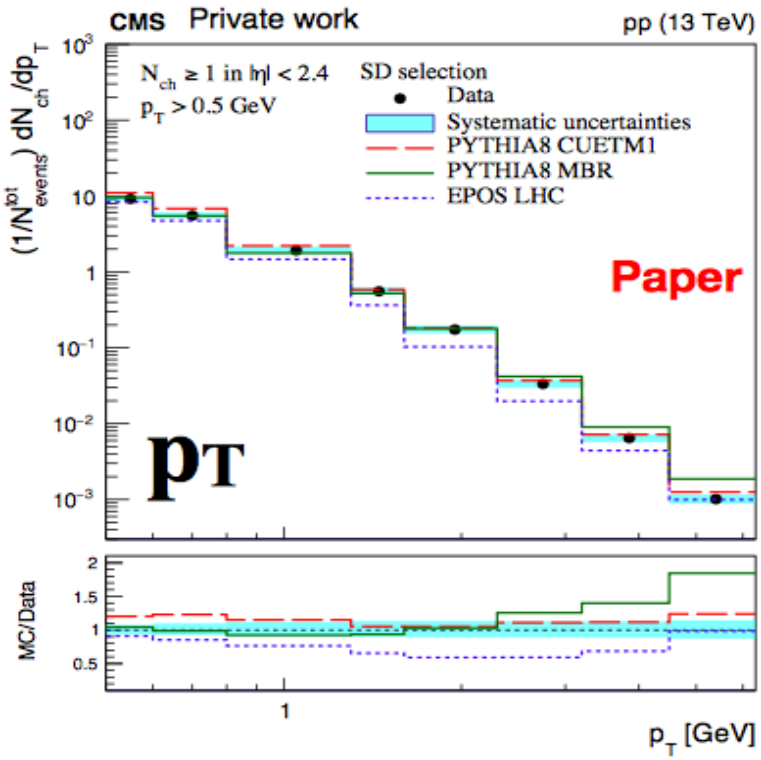

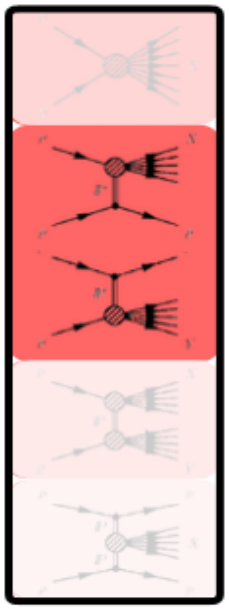

- **Overall good** description
- MBR model over estimates high p_T
- P8 CUETM1 gives **best** description

40

Model comparison

Non-SD enhanced Sample

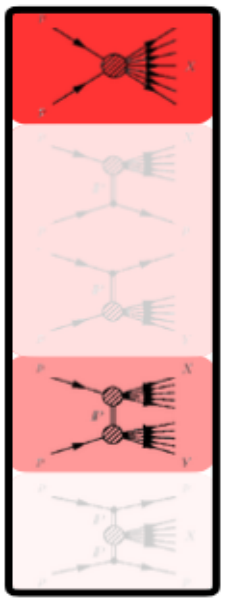

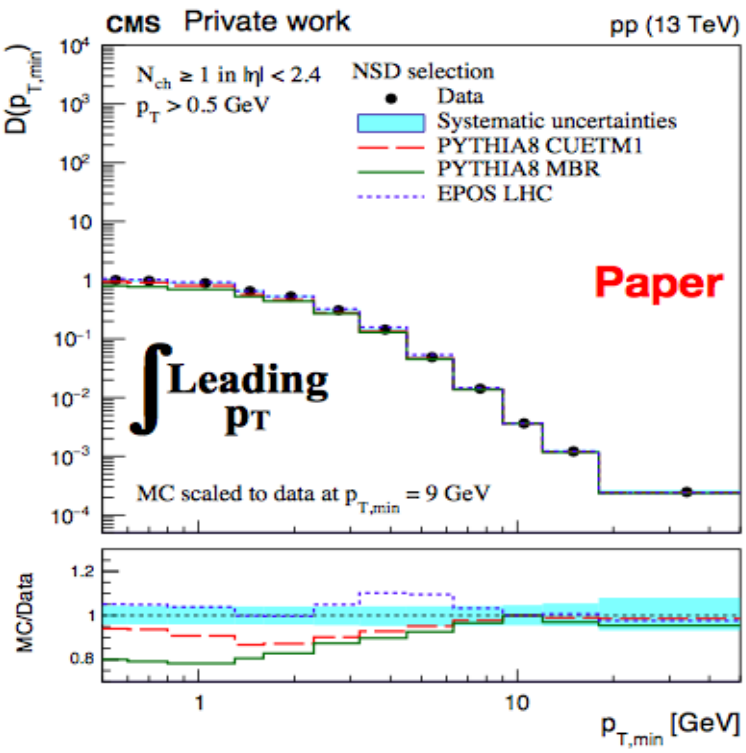

SD enhanced Sample

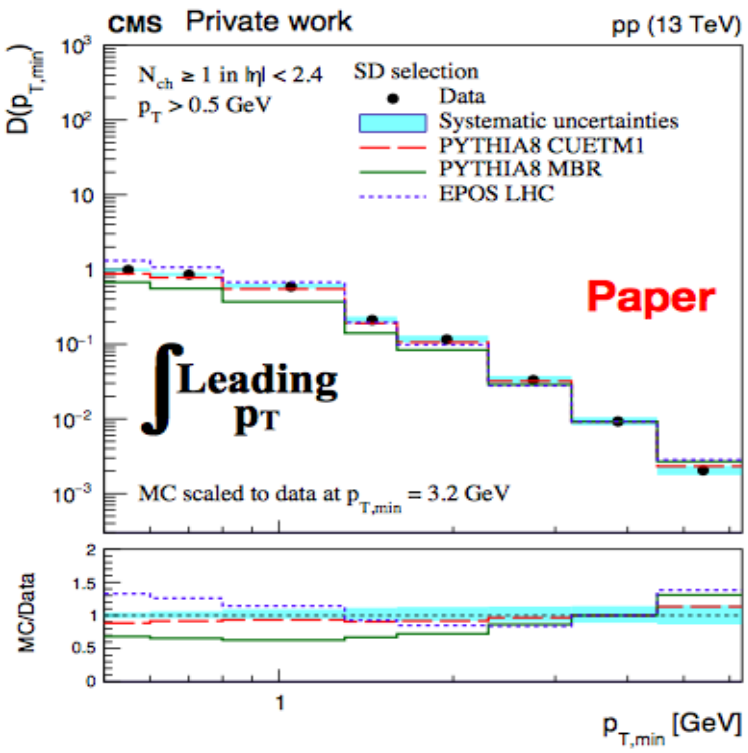

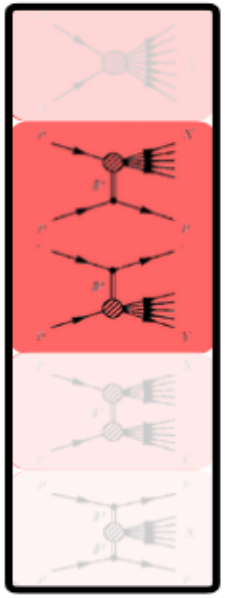

MC scaled to data at high p_T:

- **pQCD** gives more **robust** predictions

Low p_T region **difficult** to describe

- Sensitive to **saturation** and **MPI** modelling

41

Summary & conclusions

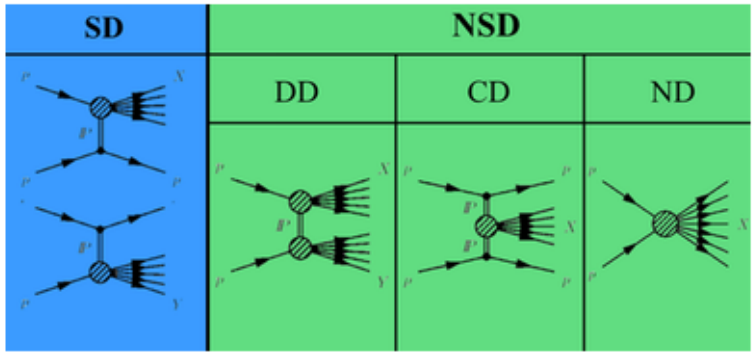

- **Unique measurements** of charged-particle spectra in **different final** states including **diffractive enhanced event samples**

- **Turnover** of integrated track distribution shows sign for taming (**saturation of x-section**)
  - Difficult region of phase space for the MCs to describe
  - Interesting to study since it is the **transition region** between **perturbative** calculations and **phenomenological** models
- Part of these results are now integrated in the **tune validation** procedure in CMS

Underlying Event (UE) Observables

Underlying Event study using Leading Track/Jet:

CMS PAS FSQ-15-007

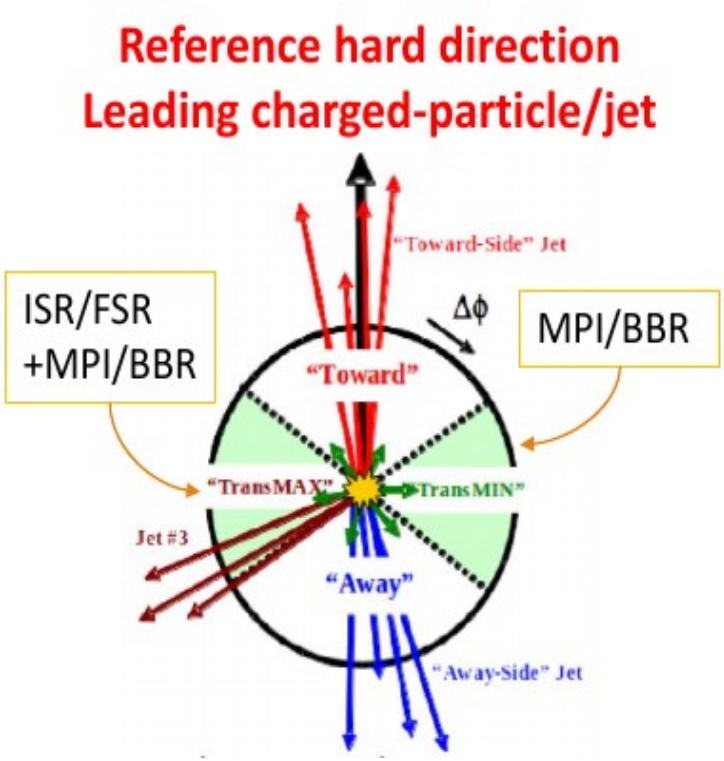

Spatial Distribution of tracks is categorized by azimuthal separation $\Delta\Phi = \Phi_{track} - \Phi_{leading\ track/jet}$

1. $|\Delta\Phi| > 120^0$ (away)
2. $60^0 < |\Delta\Phi| < 120^0$ (transverse)
3. $|\Delta\Phi| < 60^0$ (towards).

UE observable:

Avg charged particle multiplicity density:

$\langle N_{ch} \rangle / [\Delta\eta\Delta(\Delta\varphi)]$,

Average Scalar sum of transverse momenta

$\langle \Sigma p_T \rangle / [\Delta\eta\Delta(\Delta\varphi)]$

transMAX(TransMIN): activity in maximum (minimum) activity side of transverse region

transAVE: (TransMAX+TransMIN)/2

transDIF: (TransMAX-TransMIN)
Sensitive to ISR/FSR

Underlying event with leading particle and Jet @ 13 TeV

- Average p_T sum vs leading jet p_T for charged particles – p_T > 0.5 GeV and $|\eta| < 2$.

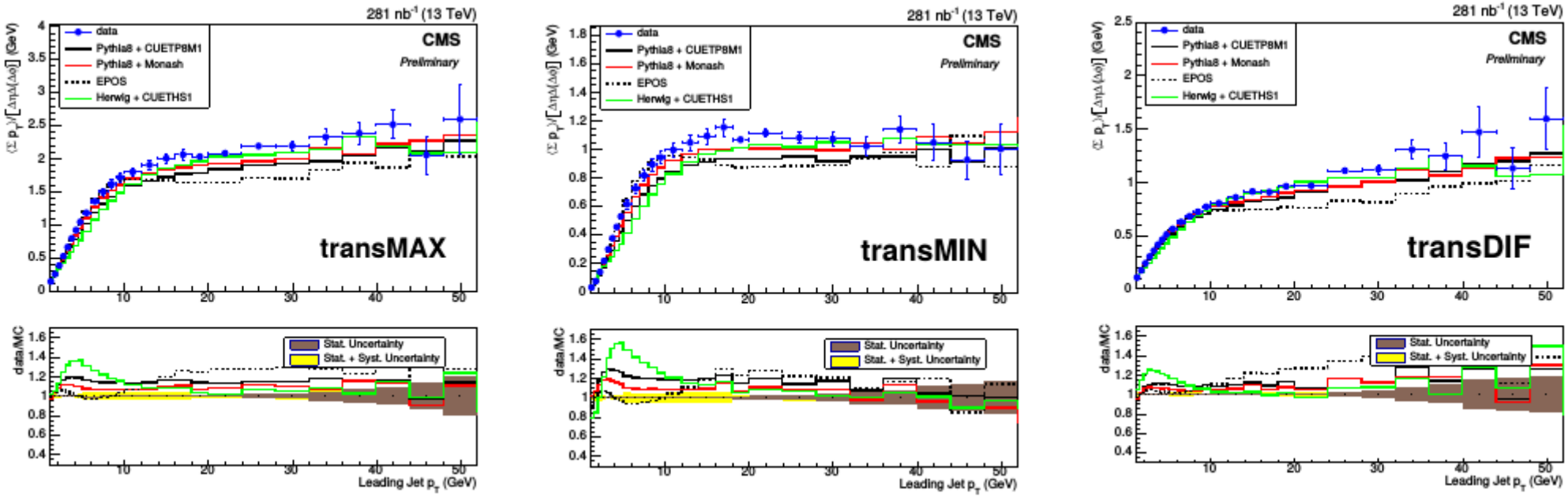

Qualitative behavior described by the simulations:

CMS PAS FSQ-15-007

- Level of agreement is 10-20% in the plateau region.
- Larger difference between models in the low p_T regions.

→ Data better described by Pythia8 Monash and CUETP8M1

HERWIG + CUETHS1 fails in the low p_T region (lack of diffractive events)

EPOS describes the rising part but fails to describe the plateau.

Underlying event with leading particle and Jet @ 13 TeV

- p_T sum density vs leading jet p_T : energy dependence 2.76 TeV → 13 TeV

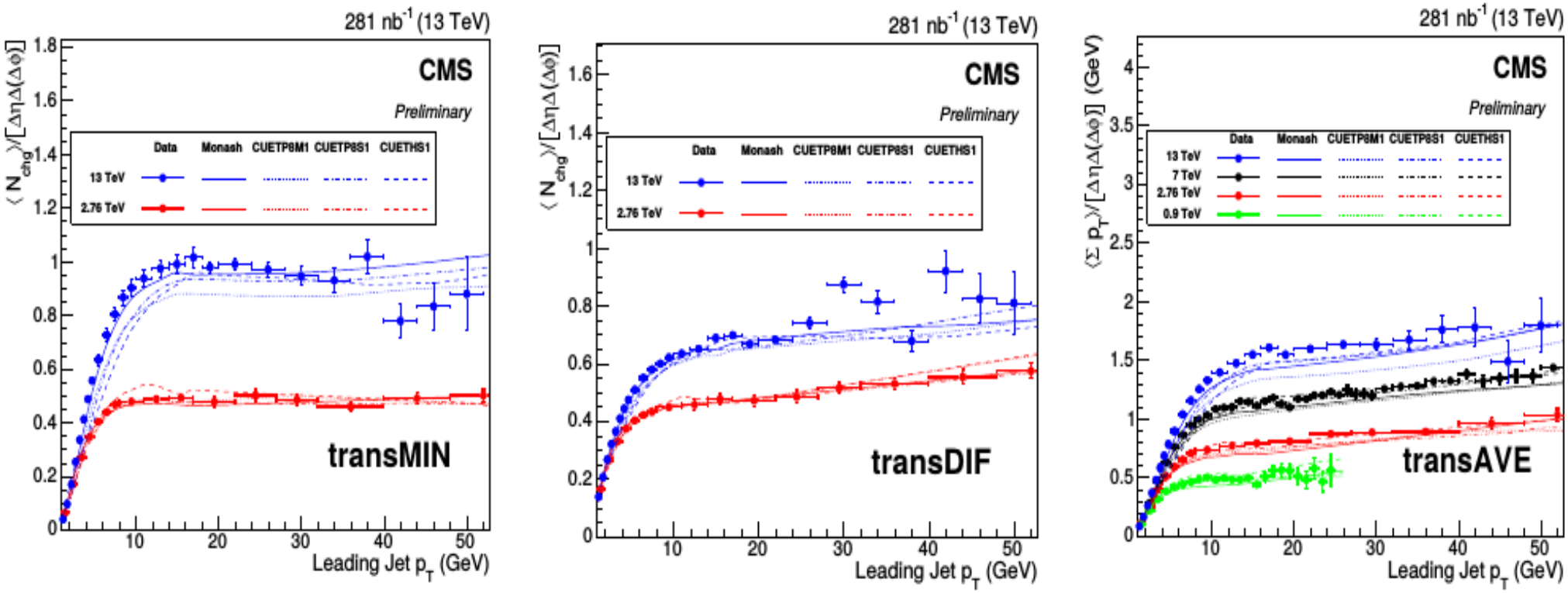

Strong energy dependence well reproduced by the different models

CMS PAS FSQ-15-007

- Increase of the parton densities at smaller momentum fraction.
- transMIN shows a stronger rise than transDIF

→ MPI activity grows faster with CM energy than activity from ISR and FSR.

Variables to characterize the UE activity

13

- **Event shape observables from the sphericity tensor**

$$S^{\mu\nu} = \frac{\sum_{i \epsilon UE} p_i^{\mu} p_i^{\nu}}{\sum_{i \epsilon UE} |p_i|^2}$$

==> S tensor has 3 eigenvalues, $\lambda_1 > \lambda_2 > \lambda_3$ with eigenvectors v_1, v_2, v_3
==> Event plane formed by v_1 and v_2
==> Particles will cluster around these two directions and that defines the event plane. In the ttbar case, the 2 b-jets are approximately correlated to these directions.

- **Aplanarity** - $A = \frac{3}{2}\lambda_3$ - measures the transverse momentum component out of the event plane, defined by the two leading eigenvectors. Isotropic (planar) events are expected to have A=1/2 (0).
- **Sphericity** - $S = \frac{3}{2}(\lambda_2 + \lambda_3)$ - measures the p_T^2 with respect to the axis of the event. An isotropic (dijet) event is expected to have $S = 1$ (0).
- **C**= $3(\lambda_1\lambda_2 + \lambda_1\lambda_3 + \lambda_2\lambda_3)$ - identifies 3 jet events (tends to be 0 for dijet events).
- **D**= $27\lambda_1\lambda_2\lambda_3$ - identifies 4 jet events (tends to be 0 otherwise).

A ==> measure of momentum along (v_1 x v_2) ~ v_3

Variables to characterize the UE activity

14

- Further insight through the evolution of the 9 observables in different categories of the ttbar system kinematics.
- Different categories chosen to be sensitive to the recoil or the scale of the hard process (and could be reconstructed with very good resolution).
  - Jet multiplicity,
  - dilepton p_T,
  - dilepton mass.
- Instead of ttbar variables, we use dilepton variables.
  - two neutrinos ==> ttbar can only be reconstructed by p_T(miss) measurement as an estimate of the total transverse momentum.
  - p_T(miss) correlated with the UE activity and has much poorer resolution.

DPS in same sign WW production

- W Boson Production: a benchmark process at LHC.
- same-sign WW DPS to leptons is very promising theoretically
  - Opposite-sign WW production cross-section via DPS is smaller than that of via SPS.
  - production cross-section for same sign WW production via DPS is comparable to SPS process.
  - very clean final state: two leptons with some missing E_T
- good process to track down correlations in proton's pdf structure!

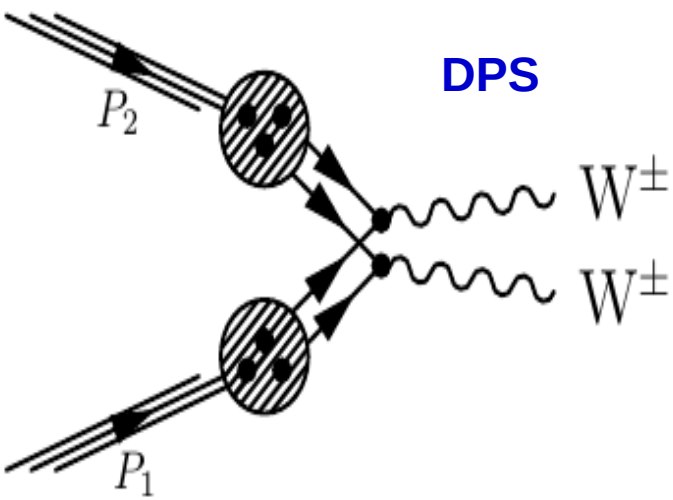

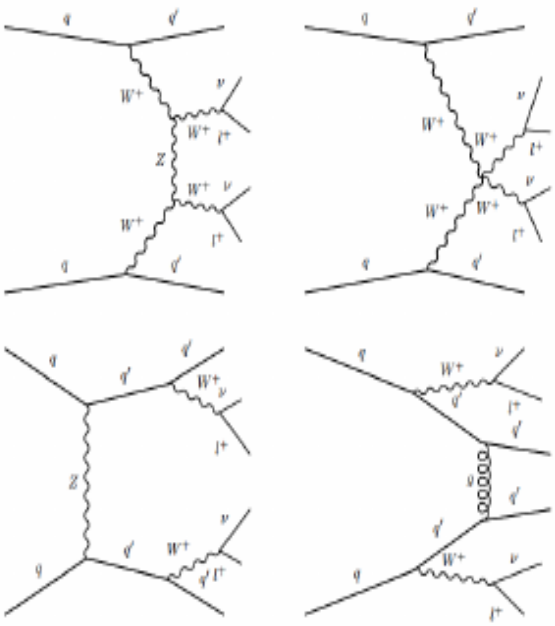

DPS in same sign WW : BDT Classifier training

CMS-PAS-FSQ-13-001

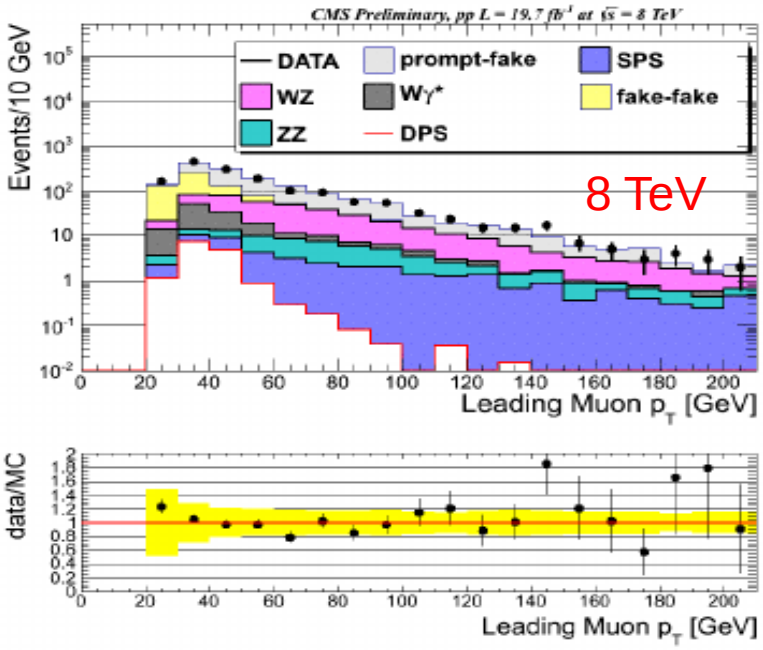

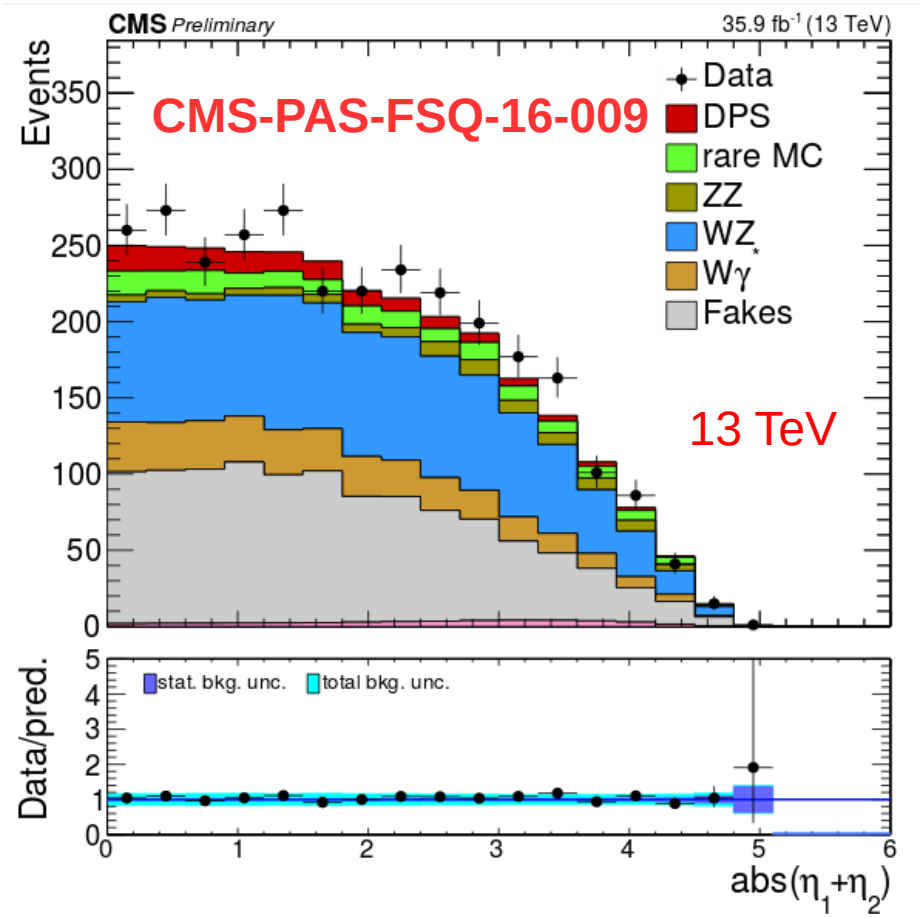

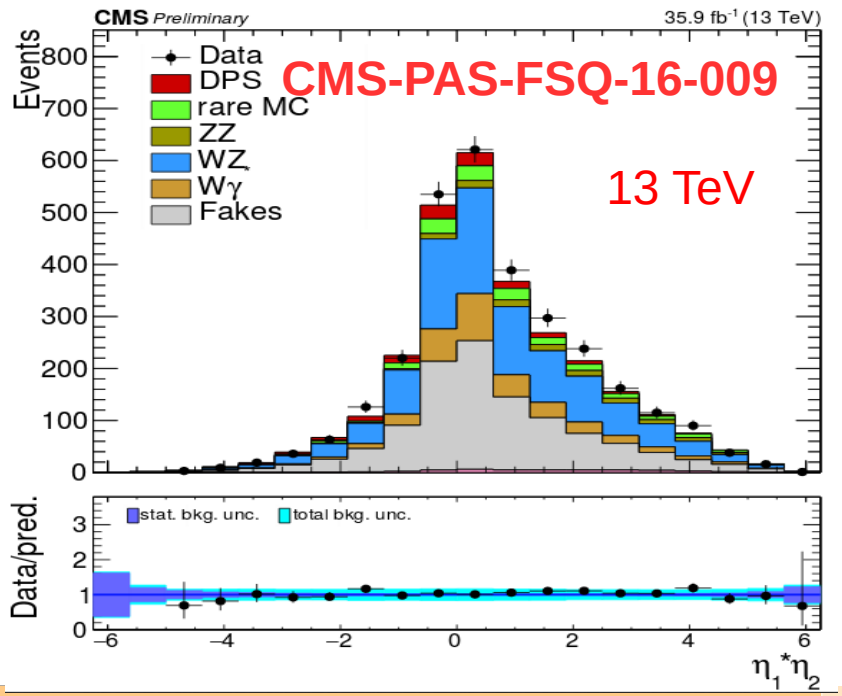

Good agreement in input variables.

Likelihood for BDT algorithm in 4 categories: $\mu^+\mu^+$,$\mu^-\mu^-$,e^+e^+,e^-e^- (for 13 TeV)

DPS in same sign WW @ 13 TeV : Results

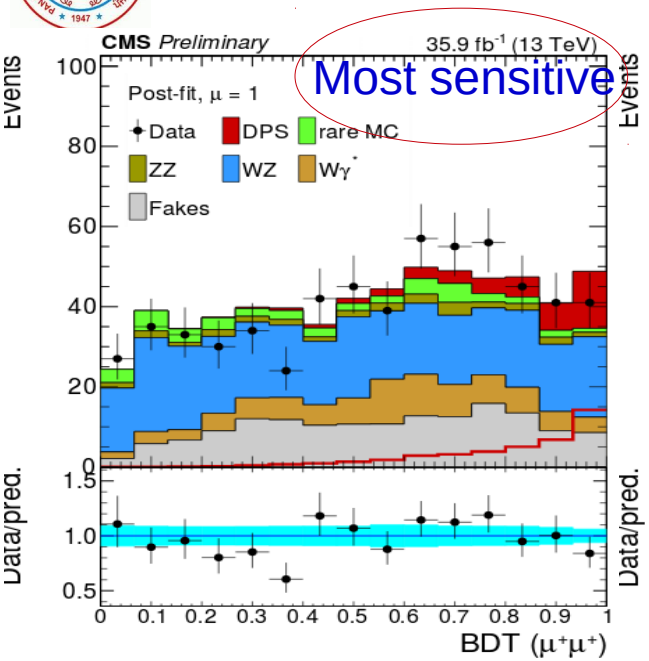

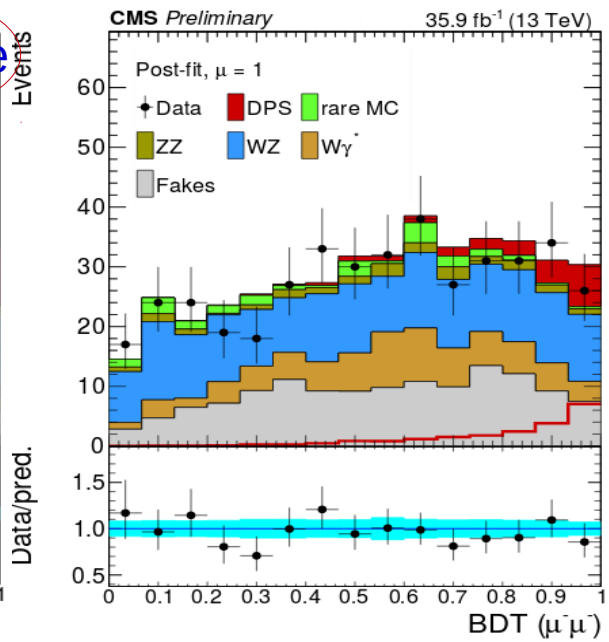

CMS-PAS-FSQ-16-009

	expected	observed
σ_{DPSWW}^{pythia}	1.64 pb	$1.09^{+0.50}_{-0.49}$ pb
$\sigma_{DPSWW}^{factorized}$	0.87 pb	
significance for σ_{DPSWW}^{pythia}	3.27 σ	2.23 σ
significance for $\sigma_{DPSWW}^{factorized}$	1.81 σ	
UL in the absence of signal	< 0.97 pb	< 1.94 pb

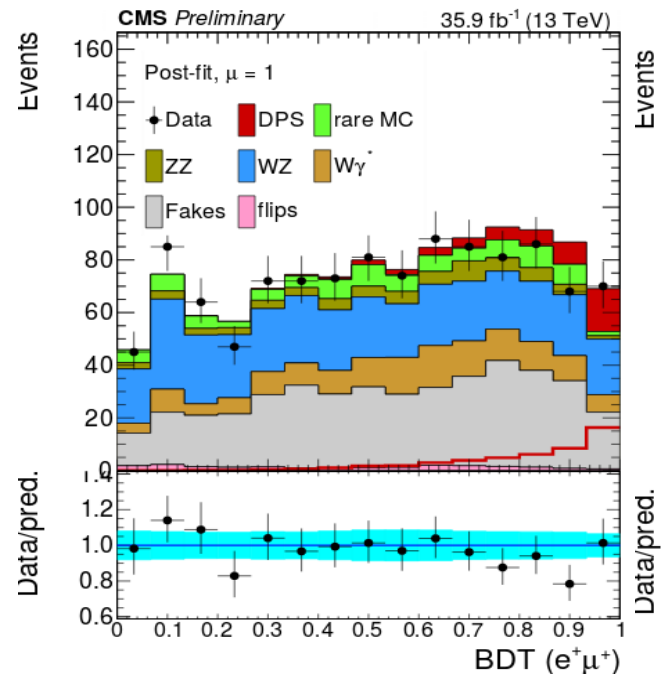

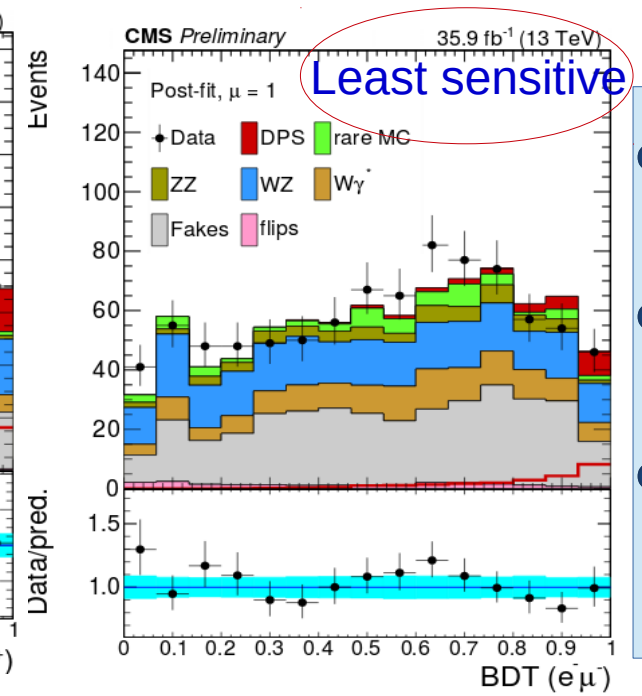

- Final BDT classifier output with all background estimations.
- Results obtained from a constrained fit to the BDT classifier.
- This result presents the most precise measurement of DPS WW process to date

Extraction and validation of a new set of CMS PYTHIA8 tunes from underlying event measurements (CMS PAS GEN-17-001)

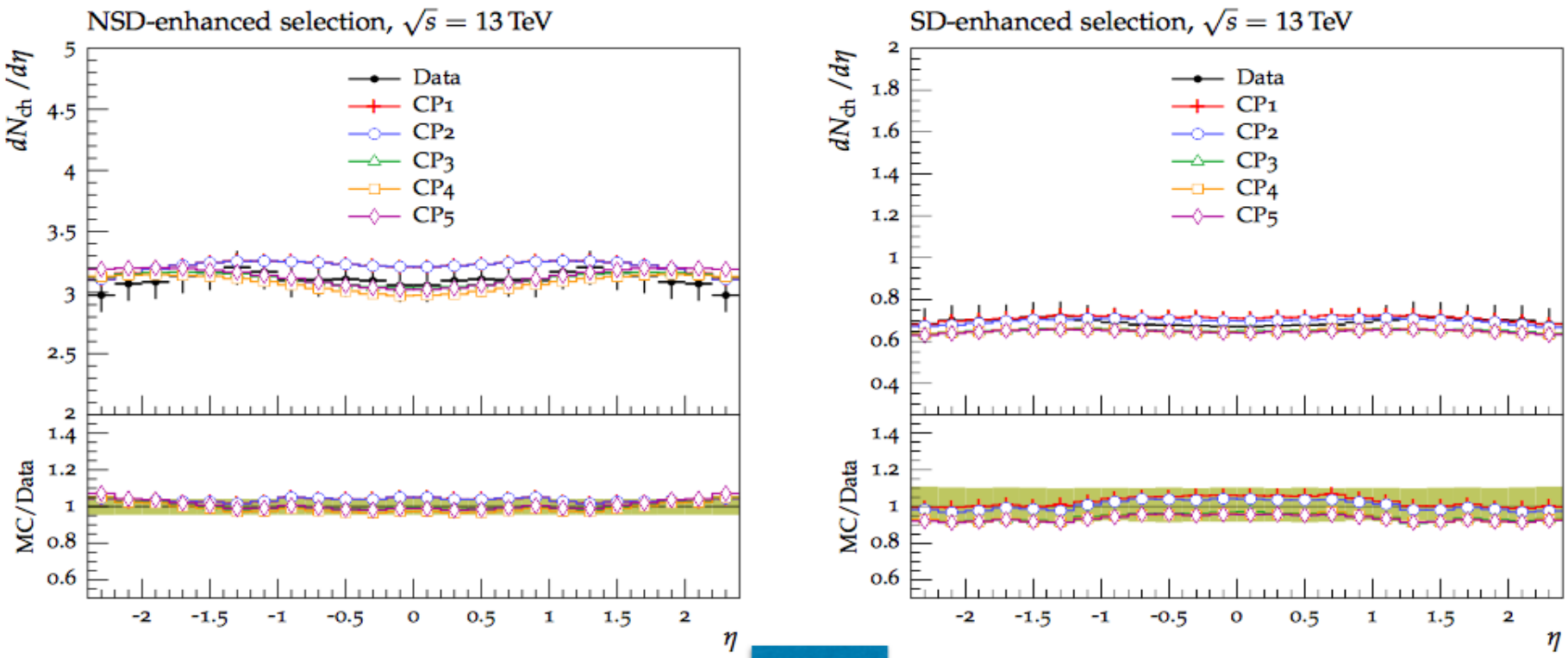

paper

- new CMS tunes simultaneously describe the number of charged particles produced in NSD- and SD-enhanced processes and inelastic collisions.
- tunes based on NNPDF3.1 PDF sets at orders higher than LO adequately describe the MB data.

Extraction and validation of a new set of CMS PYTHIA8 tunes from underlying event measurements (CMS PAS GEN-17-001)

CP5 and strong coupling values

27

- ISR/FSR variations studied to check the consistency of the selected strong coupling values for the tunes.
- Starting from CP5, $\alpha_s^{ISR}(M_Z)$ is fitted to UE observable measured by CMS at 13 TeV.
- Starting from CP5, $\alpha_s^{FSR}(M_Z)$ is fitted to UE observable measured by CMS at 13 TeV.

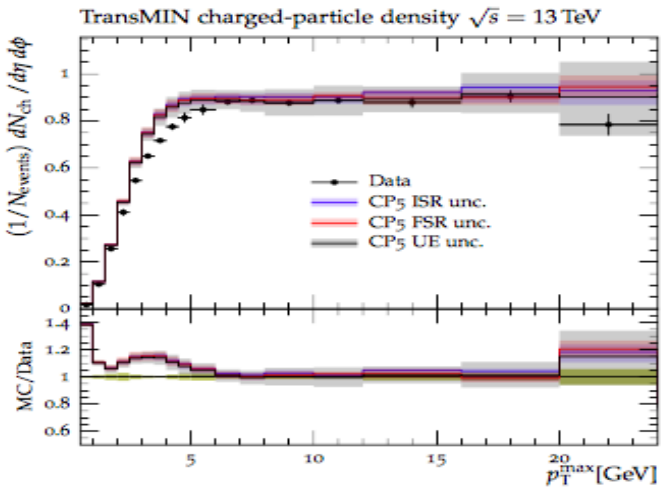

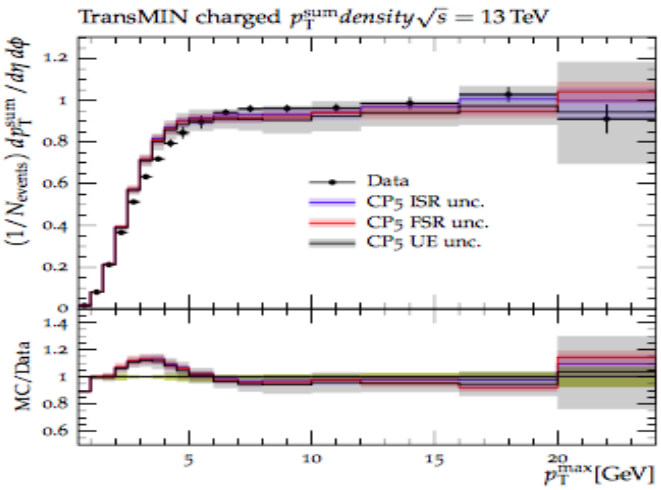

paper

Table 7: "UP" and "DOWN" ISR and FSR variations for CP5 when $\alpha_s^{ISR}(M_Z)$ or $\alpha_s^{FSR}(M_Z)$ is treated as a free parameter.

PYTHIA 8 Parameter	Central	Up	Down	χ^2/dof
$\alpha_s^{ISR}(M_Z)$ value	0.1213	0.1276	0.1145	0.749
$\alpha_s^{FSR}(M_Z)$ value	0.1186	0.1219	0.1152	0.775